3.0   METHODOLOGY FOR REACTOR PHYSICS ANALYSIS IN CORE DESIGN

3.1   Summary

This Section will give a very brief overview of the typical methodology used in the process of designing a CANDU reactor core. The intent is to set the stage for the discussion that will follow where the methods that are used and the reasons for using them will be discussed in more detail.

Figure 3.1-1[6] gives a simple flow chart of the physics analysis of CANDU power reactors. The activities involved in the various stages are outlined below:

3.1.1   Engineering Requirements

The establishment of the broad engineering requirements of the core design will depend on the nature of the design and the project. If a new reactor design concept is involved, considerable interaction between reactor physics analysis and the engineering design consider-ations would take place during the establishment of the conceptual design of the plant. On the other hand, if the project is a relatively small variant from the reactors previously designed, the basic engineer-ing requirements may be established on the basis of past experience with minimal "conceptual" work being done. In any case, before the detailed reactor physics analysis of a core design can begin, a preliminary selection of a number of key parameters is required. These include the size of the core, number of channels, the design of fuel channel and fuel bundle, the required operating conditions, preliminary choices of material to be used in the core hardware, etc. Some of these parameters may well change as a result of the physics analysis and hence an iter-ative process take place in order to satisfy both engineering and physics requirements.

3.1.2   Lattice (Cell) Calculations

In a lattice calculation, a unit cell consisting of a single fuel channel and the appropriate amount of moderator (depending on the pitch) is considered. The lattice calculation provides neutronic details of the fuel channel. In particular, it provides information on the variation of cross sections and isotopic composition with fuel burnup, the reactivity coefficients, the power distribution across the fuel bundle, and the macroscopic cross sections to be used in core calculations.

3.1.3   Simulation Of Reactivity Devices

Due to the large number of reactivity devices present in the core, they are generally not represented discretely in the core simulations. Rather, the properties of a device are smeared over a fairly large parallelepiped one dimension of which is the length of the device. These properties are usually obtained by what is known as a supercell calculation, which must be done for each different device.

3.1.4   Core Calculations

When the cell average cross sections and the incremental cross sections for the reactivity devices are available, core calcula-tions can be carried out. Finite difference diffusion codes are used for these calculations, in two neutron energy groups. The number of mesh lines used in the finite difference models depends on the nature of the problem being dealt with. In some cases two dimensional calculations are adequate, but three dimensional models are necessary to estimate accurately the power distributions in CANDU reactors.

3.1.5   Kinetic Studies

Transient behaviour of the reactor may be studied either using a point kinetics approach or complete three dimensional simulations in both space and time. The latter is important in the final confir-mation of performance of the shutdown systems.

3.1.6   Reactor Stability And Control

Detailed design of the spatial control system (one purpose of which is to control the spatially variable distribution of ^{135}Xe) requires a diffusion code with the capability to calculate the variation of xenon concentration in space and time. In addition this code must be able to simulate response of the spatial control system to spatial flux variations caused by perturbations such as withdrawing of adjuster rods or refuelling.

3.1.7   Fuel Burnup And Management

Obtaining optimum average discharge burnup of the fuel is an important aspect of the physics design of the reactor. This requires a diffusion code which is capable of calculating the time history of the flux and power distributions in each fuel bundle from any particular starting point and time. However the bi-directional feature of fuelling in CANDU reactors permits an averaging of fuel properties so that conceptual studies can be done with much simpler models.

3.1.8   Flux Mapping

A computer code based on modal analysis is used to simulate the flux mapping software which is incorporated in the reactor control computer so that the positions of the flux mapping detectors can be optimized during the design stage.

Figure 3.1-1 also illustrates the interdependence of these various analyses as well as some functions of the specific computer codes that are used.

3.2   CANDU PHYSICS METHODOLOGY

3.2.1   Introduction

In the preceding Section we briefly touched on the scope of physics analysis that typically takes place in the process of designing a CANDU reactor. In the next Section we will be dealing with this process in detail and discussing some of the typical results we obtain from our analysis. Therefore, the objectives are basically two-fold: firstly to provide an understanding of the methods we use, and secondly to give a fairly detailed description of the physics characteristics of these reactors. The organization of the next several Sections is based on the intent to follow a typical sequence of activities which take place in the process of performing the reactor physics analysis required to produce a CANDU reactor design.

3.2.2   Conceptual Stage Design Analysis

In the most general sense the conceptual stage of a reactor design begins with determining the broad conceptual features of the reactor. However for purposes of these lectures we will begin with the premise that the intent is to design a pressure tube type reactor with heavy water used for both moderator and coolant and the latter is either non-boiling or at very low quality at the outlet of the channels (less than 5% quality).

The basic building block of the CANDU pressure tube type reactor is the fuel channel. The design of the fuel, pressure tube, and the calandria tube and the separation of these assemblies from each other (which will be referred to hereafter as the lattice pitch) determine the basis nuclear characteristics of the reactor core. Since there is a repeating array of these assemblies throughout the core, the basic nuclear characteristics can be determined by considering only one channel surrounding by the appropriate volume of heavy water moderator. This is commonly called a "unit cell" and is shown in Figure 3.2-1. The nuclear characteristics of a unit cell are called lattice parameters.

3.2.2.1   Calculation Of Lattice Parameters

There are a number of methods which are used to determine the reaction rates within a unit cell. In all of these calculations the boundary condition at the outer surface of the moderator associated with the unit cell is taken to be zero gradient of the neutron flux (no leakage of neutrons). The method which is applied in the unit cell calculation depends on the detail with which the reaction rates within the unit cell need to be known. For most purposes in the process of performing the nuclear design analyses it is sufficient to know the reaction rates within the fuel bundle as a whole. Since the early days of the design of CANDU prototypes it was considered desirable to develop a fast and reasonably accurate cell code that could be used for survey and design purposes. This culminated in development of the lattice parameter program POWDERPUFS which is the code most widely used to generate the lattice parameters needed for commercial core design and analysis.

3.2.2.1.1   Functional Description Of Lattice Parameter Programs

In the POWDERPUFS code the cell is treated in a very simple manner: it is assumed to be divided into three main regions: 1 - a fuel region, 2 - an annuli region (including the pressure tube and calandria tube and the gap between them) and 3 - a moderator region. Therefore the flux distribution in the cell is calculated using a simple one dimensional annular model. This means the moderator region is approximated by circular outer boundary rather than a square as shown in Figure 3.2-1. The nuclear cross sections for the fuel are based on the Wescott convention, i.e. on the assumption that the neutron spectrum consists of a Maxwellian and a 1/e part characterized by two parameters which are calculated in the program. The resonance integrals are based on a semi-empirical treatment which agrees with Hellstrands experiments[7], and the resonance absorption is lumped into a single adjusted energy. Thermal absorption is calculated by a simple collision probability method. A complete cell calculation using this code takes only approximately one second on a CDC-6600 computer.

The calculations within this code are basically recipe type or semi-empirical type calculations which have been developed on the basis of fitting an extensive series of experiments which have been performed in the ZEEP and ZED-2 reactors at CRNL in which lattices with a range of bundle geometries and pitches have been measured. The ratio of moderator to fuel in a CANDU lattice is such that over 95% of neutrons in the moderator are thermalized i.e. have an energy distribution in equilibrium with the moderator atoms. The majority of neutrons absorbed are, therefore, thermal neutrons and the epi-thermal neutron absorption is conveniently grouped with thermal absorption using measured thermal-to-epi-thermal reaction rate ratios (an exception is resonance absorption in ^{238}U as described below). This convention is due to Wescott[8].

Neutron absorption in ^{238}U at the higher resonance energies is treated specifically and hence is not included in the Wescott cross sections. The total epi-thermal cross sections are measured in an experimental reactor and empirical expressions are derived based on data for various fuel geometries and fuel temperatures. The forms of the expressions used for the correlations have been well established and their adaptation to CANDU lattices is described by Critoph[9]. While this method is quite simplified it does provide reliable results for lattices in the range of interest for natural uranium CANDU reactors. Some of the comparisons with experimental data is shown in Figures 3.2-2 to 3.2-13 for 28 and 37 element fuel bundles. An exhaustive series of experiments have been performed with 28 element fuel in the ZED-2 reactor over an extended period of time. The 37 element fuel characteristics are similar, so only limited measurements were made in that case.

In addition to being able to generate nuclear reaction rates in the unit cell, for core calculations, it is also necessary to calculate the power distribution within a fuel bundle in order to perform the detailed fuel design. This is because an important consideration in fuel design is the maximum heat flux produced in any one pin in the fuel bundle. The POWDERPUFS code is not designed to provide detailed

power distribution data in the fuel cluster. This kind of information can be obtained from the LATREP lattice parameter program[10], or obtained directly from experimental data. The flux distribution is calculated in LATREP at several energy groups using collision probability methods. Resonance integrals of fertile materials are based on semi-empirical recipes but the resonance absorption is calculated in 32 groups. A single thermal group is assumed, however, using the Wescott convention for reaction rate calculations in non-fertile isotopes and in fissile isotopes.

In this code the fuel pencils are smeared into annular rings so that the reaction rates can be calculated separately in each of these rings and from those results the power distribution across bundle can be determined. Although it is a one dimensional calculation the comparisons of this method against experiment is shown to be reliable[1][11].

Although POWDERPUFS and LATREP are the codes routinely used in CANDU core design analysis, we also apply multi-group transport codes such as WIMS[12] and HAMMER[13], primarily to perform spot checks for these simpler and much faster codes. A series of transport codes have also been developed at AECL. An R-Z code (PEAKAN)[21] is used primarily for treating the bundle-end flux peaking problem described by Critoph[1]. An X-Y-Z code (SHETAN)[23] is used to calculate reaction rates in interstitial absorbers (or boosters) of complex geometry. GETRANS[20] is a two dimensional version of SHETAN.

There are also certain specific problems where even the so-called "hyperfine" distribution of flux within the fuel pin is important to determine. This requires the use of multi-group codes. One such example is the importance of knowing the detailed pin power distribution in estimating fission gas generation during irradiation. We have found an important difference in the variation of the hyperfine pin power distribution with irradiation between the natural uranium fuel and enriched fuel. This was discovered as a result of investigations

to understand why fission gas releases from fuel in our operating
reactors seemed to be inconsistent with detailed experimental measure-
ments done in the research reactors at Chalk River. In the latter case
fuel is normally enriched in order to get the power densities that are
desirable for testing purposes. We find that, because of the so-called
"skin effect", resonance absorption occurs preferentially at the surface
of the pin. The corresponding preferential plutonium production as the
irradiation proceeds tend to cause a relatively larger proportion of
power to be produced near the surface of the pin for irradiated natural
fuel than for irradiated enriched fuel. (In the latter case the contri-
bution of plutonium to the total energy produced in the pin is much
smaller.) This is illustrated in Fig. 3.2-12.

        The degree of sophistication of analytical methods used
to perform unit cell calculations depends on the problem being dealt
with. Our approach is to apply the multi-group codes only in those
cases where their capabilities are demanded.

3.2.2.1.2 Special Features For CANDU Applications

        For conceptual design studies, the POWDERPUFS code is
used to generate lattice parameters for various fuel geometries and
pressure tube and calandria tube characteristics and also for various
values of lattice pitch. Average cell parameters are produced for each
case. These parameters are then put into a diffusion code to simulate a
reactor core. In fact the POWDERPUFS code has built within it the
capability to perform a simple one dimensional analytical core calcula-
tion in which fuel can be assumed to be at different burnups in annular
regions in the core and the heavy water reflector surrounding the fuel
channels can be simulated. This is convenient for the very early
conceptual stages of a design study as the fuel burnup achievable for
various core sizes and various degrees of radial flattening in the core
can be examined as well as the effect of changing reflector thickness
all at very minimal cost.

Many other features have been added to the POWDERPUFS code to make it very useful to obtain a lot of the data that is important to evaluate nuclear characteristics of the CANDU reactors without having to perform the full core modelling type of calculation with diffusion codes.

A feature which is important in respect to treating the bi-directional semi-continuous fuelling that occurs in a CANDU reactor at equilibrium burnup is the capability to average reaction rates over a burnup interval. The basic output of POWDERPUFS, as with most other cell codes, are the cell-average lattice parameters (in this case cross sections in two energy groups) as a function of the irradiation seen by the fuel. However if we consider two adjacent channels in the CANDU reactor and assume ideally that they are being fuelled continuously in opposite directions, each channel would have fuel with irradiation ranging from zero to the discharge value from one end of the channel to the other. We find that if we calculate average reaction rates by integrating over this irradiation interval, the corresponding lattice properties are not very different than what would be obtained if the properties of two adjacent channels are averaged point by point along the channel.

This feature provides a very convenient way to calculate lattice parameters for a reactor operating under equilibrium fuelling conditions for any given assumed discharged burnup. These average parameters can be calculated within the POWDERPUFS program. The methodology by which these average properties are determined is discussed in more detail in the course on CANDU-PHW Fuel Management [23].

Another feature of the program which is very useful, is the capability to calculate the effect on these averaged properties of instantaneously changing the characteristics of the materials in the fuel channel e.g. changing fuel temperature, coolant temperature, coolant density, removing coolant completely etc. This feature is used to determine reactivity coefficients for the reactor during the concep-

tual stage, and in some cases the POWDERPUFS calculations are sufficiently accurate for the final design.

In addition to giving the cell averaged cross sections used in two-group diffusion code simulation of the reactor core, the POWDERPUFS program also provides the classical "four factors" which determine the multiplication factor for the infinite lattice. The effective multiplication factor for a finite core having a given geometric buckling is also calculated as indicated in the following equations:

$$k_\infty = \eta \varepsilon p f$$

$$k_{eff} = \frac{k_\infty}{(1+L^2 B_g^2)(1+L_s^2 B_g^2)}$$

Note that the expression for effective multiplication factor includes terms which account for the leakage from a finite core for which the effective geometry buckling is B_g^2, an input quantity. This is valid, to the extent that this buckling can be estimated for a "real" system. The calculated k_{eff} when based on reaction rate averaged cross-sections, gives a reasonable estimate of the multiplication factor of a reactor as a function of discharge burnup. This means that the POWDERPUFS code alone can be used to study sensitivity of discharged fuel burnup to changes in the fuel channel design characteristics and operating temperatures. It can also be used to determine the impact of these changes on the reactivity coefficients which are important from the point-of-view of control and shutdown system implications. This is important in both the conceptual and detailed design stage as a large number of parameters variations can be studied at relatively small expense. In fact the POWDERPUFS program has been incorporated into a comprehensive optimization program which considers all the other economic aspects of various design changes and arrives at a total unit energy cost for a given system.

Some of the things which are "traded-off" in this optimization process are: the capital cost savings in minimizing the number of channels and the size of the calandria are balanced against increased fuelling cost associated with the need to flatten the power distribution to achieve the required energy output with a smaller reactor (because of increasing the neutron leakage from the system); reducing the pitch of the fuel channels saves capital cost because of reducing the size of the calandria and the heavy water inventory but that would result in lower burnup and introduce design complications in respect to (a) the spacing of feeders from each channel and (b) constraints imposed on the control and shutdown system devices which have to be provided interstitially. Many other variables are, of course, examined as well.

It is this kind of process which has led to the evolution of the CANDU PHW design from the smaller channel and 19 element fuel bundles in NPD and Douglas Point to the larger channel and 37-element fuel bundles in the current generation reactors. The change from 28-element fuel to 37-element fuel in the same size channel in going from Pickering to the reactors which followed it was also based on this kind of optimization process. The greater fuel sub-division permits each channel to operate at a higher power for a given fuel pencil rating and hence reduces the number of channels required in a given size of core. This, however, is at the expense of fuel burnup to some degree.

The basic fuel channel design including the fuel is generally arrived at by applying this optimization analysis using simple cell calculations to determine nuclear characteristics of the reactor with some one dimensional core simulations done to properly account for the effect of changing the radial power flattening and/or the reflector thickness on the reactor dimensions and fuel burnup.

3.2.2.2   Typical POWDERPUFS Calculations For The CANDU-600

3.2.2.2.1 Four-Factor Data

Figure 3.2-13 show the infinite multiplication factor

versus neutron irradiation of the fuel. The variation of the parameters
η (neutrons produced per thermal neutrons absorbed) and f (thermal
utilization) with irradiation are also shown. The other two parameters
ε (fast fission factor) and p (resonance escape probability) are
essentially constant with irradiation. Note that the thermal utilization
is also almost constant with irradiation. This shows that the absorp-
tion cross section of the fuel which is dominated by the heavy elements
changes very little tending to increase slightly with irradiation. This
is because the buildup of plutonium isotopes due to capture in ^{238}U just
about balances the burnout of the ^{235}U. The η variation is very similar
to the overall multiplication factor. The decrease with irradiation is
primarily because of the buildup of fission products in the fuel.

3.2.2.2.2 Fuel Temperature Reactivity Effects

The fuel temperature reactivity coefficient is shown
versus instantaneous irradiation* in Figure 3.2-14. Note that it is
significantly negative with fresh fuel and becomes less negative with
irradiation. The value labelled "reaction rate averaged" which also is
shown on this Figure is the value calculated using reaction rate
averaged parameters for the irradiation which is typical of the average
discharge from the reactor. It is plotted at an irradiation equal to
half of the discharge irradiation to permit comparison with the "instan-
taneous" data. (In a continuous bi-directionally fuelled reactor the
average irradiation of fuel in the core would be half of the discharge
value).

The effect of heating up the fuel from low temperature to
the operating temperature is shown in Figure 3.2-15. Again the differ-
ence between an irradiated fuel and fuel at equilibrium burnup conditions
is evident. Also note that the variation is more non-linear with
irradiated fuel. This is related to the effect of changing the neutron
spectrum with plutonium isotopes present in the fuel.

---

*This term refers to the actual irradiation experienced by an individual
fuel bundle in the core. "Instantaneous" is used to distinquish between
actual local irradiation and an average irradiation of a larger number
of bundles which is useful in considering overall core characteristics.

3.2.2.2.3 Coolant Temperature Reactivity Effects

The effect of instantaneously changing the coolant temper-
ature on the reactivity of fuel varies with irradiation as shown in
Figure 3.2-16. This was calculated assuming that the coolant density
changed with temperature in a manner consistent with retaining saturated
conditions. The point calculated at the average discharge burnup for
the equilibrium burn-up reactor using the reaction rate averaged cross
sections is also shown on this Figure.

The variation of reactivity with coolant temperature
changing from a low value to the operating temperature is shown in
Figure 3.2-17. Note that although the coefficient (i.e. the slope of the
curve) is positive at the operating temperature for both fresh and
irradiated fuel, it is quite nonlinear for fresh fuel and in fact
changes sign at low temperatures. There are two counter-balancing
effects which take place as the temperature for the coolant is raised.
The effect of making the coolant hotter than the moderator (which is
typically kept at around $70^{\circ}C$) tends to harden the neutron spectrum in
the fuel since the hot coolant speeds up thermal neutrons coming from
the moderator. On the other hand since the coolant density is decreasing,
this spectrum hardening effect is less than it otherwise would be.
(Changing the spectrum affects fuel with plutonium isotopes present much
differently than that with ^{235}U only. Therefore, the irradiated fuel
behaves quite differently than the fresh fuel.) Another phenomenon that
occurs when the coolant density is reduced is that the resonance absorp-
tion in ^{238}U decreases. This is because having coolant within the fuel
cluster tends to slow more fission neutrons down through the resonance
region as they are leaving the fuel and hence increase the flux of
resonance neutrons within the cluster.

3.2.2.2. Loss-of-Coolant Reactivity Effect

Rupture of the primary heat transport system, although
highly improbable, is one of the accidents which is postulated in design
of the reactor safety systems. Since this accident leads to loss of

coolant from some or all of the fuel channels the magnitude of this effect on reactivity is an important design parameter. Figure 3.2-18 shows the reactivity effect of simultaneously losing the coolant from all fuel channels for various fuel irradiations. Again the value for the equilibrium fuel case using reaction rate averaged parameters is shown on the same Figure.

Reactivity change due to losing the coolant is positive but not very large in magnitude and decreases with fuel irradiation. As mentioned in the preceding Section, reducing coolant density results in an increase in the resonance escape probability due to lower resonance energy flux in the cluster. However, because the coolant is hot under normal steady state full power conditions, it tends to harden the spectrum of thermal neutrons coming from the moderator, which is a positive reactivity effect when plutonium is present in the fuel. When the coolant is lost this hardening effect no longer exists which results in a decrease in reactivity, the magnitude of which is function of the concentration of plutonium isotopes in the fuel. This is why the loss-of-coolant reactivity decreases with fuel irradiation.

3.2.2.2.5 Moderator Temperature Reactivity Effect

The moderator temperature is not a parameter of much significance in the CANDU system because the moderator is essentially completely isolated from the fuel channel and the temperature of the moderator is relatively low and separately controlled. However it is of interest to know the reactivity effect associated with instantaneous changes in the moderator temperature to assess the impact on the reactor of changes that may occur due to upsets in the temperature control system of the moderator. The moderator temperature coefficient is plotted versus fuel irradiation in Figure 3.2-19. A reaction rate averaged point is also shown on this Figure.

3.2.2.2.6 Reactivity Effect Of Boron In The Moderator

Adding "poison" in the form of dissolved natural boron or gadolinium to the moderator is the usual way of compensating for excess reactivity which exists when the reactor is initially loaded with all unirradiated fuel or during operation at equilibrium burnup when the reactor has been shut down for a significant period so that the ^{135}Xe in the fuel has decayed away. Therefore, the reactivity effect of changing the boron concentration in the moderator is a necessary design parameter. The effect of instantaneously changing the boron concentration for various fuel irradiations is plotted in Figure 3.2-20. In this case the calculations were done with reaction rate parameters for all cases. Note that the coefficient is not very dependent on the irradiation (the ordinate is an expanded scale).

3.2.3   Core Design Analysis

3.2.3.1   Core Size Considerations

Once the design of the fuel, pressure tube, and calandria tube assembly, and the spacing or pitch of the fuel channels is decided, the work associated with determining the detailed characteristics of the reactor core is undertaken. One of the first major parameters to be established is the number of channels. It is dependent primarily on the average-to-maximum channel power ratio which is obtained as the result of the optimization process discussed previously or on the basis of past experience combined with specific conditions pertaining to the project at hand.

The CANDU design theoretically permits adjusting the reactivity of each individual channel over quite a large range by altering the fuelling rate and hence changing the average irradiation of the fuel in the channel. This allows a great deal of flexibility in flattening the power distribution radially by fuel mangement alone.

In reactors such as Douglas Point and Bruce A, which have very little adjustable absorbing material in the core during normal full power operation, virtually all of the radial flattening necessary to achieve the design value of the average-to-maximum channel power is accomplished by fuel management.

During the design process the analysis is usually simplified by assuming there are only two "burnup regions" in the core. Fuel in a central region roughly cylindrical in shape is assumed to be taken to the irradiation which would give the multiplication factor only large enough to provide for axial leakage of neutrons. The fuel irradiation in the outer annular region is then adjusted to that value necessary to have a critical reactor. All channels within a region are assumed to have the same discharge burnup so the whole region can be represented by the same reaction rate averaged lattice parameters.

All the current generation CANDU reactors, after Bruce A, are designed to have an array of absorbers called adjuster rods in the core during normal full power operations so they can be withdrawn to provide excess reactivity to compensate for the buildup of ^{135}Xe following a short shutdown. In these designs the flattening of the power distribution is accomplished by fuel management combined with carefully choosing the positions for the adjuster rods. The number of channels in cores having adjuster rods is generally not finalized until 3-dimensional core simulations are done which permit explicit simulation of the effect of the adjuster rods on the power distribution. With adjuster rods in the core it is also relatively easy to flatten the power distribution axially as well as radially. If the power output of the reactor were limited by the peak bundle power rather than by the peak channel power i.e. fuel rating limited rather than because of thermohydraulic conditions in the channel, the number of channels in the reactor could be influenced by this capability to axially flatten the power distribution.

3.2.3.2 Core Design Methodology

3.2.3.2.1 Numerical Modeling Of The Core

To establish the number of channels in the reactor and
the design of the in-core reactivity devices it is necessary to perform
3-dimensional simulations of the reactor power distribution. Experience
has shown that there is no advantage in performing analysis of CANDU
cores in more than two energy groups. This has made it possible to
model the cores fairly accurately in 3-dimensions with small computing
time. Models normally use one mesh point per fuel bundle except in
regions where there are large flux gradients, e.g. near reactivity
devices. In such case the perturbed region is treated separately in
detail by doing a "super cell" calculation of that local region in which
appropriate boundary conditions can be put on the reactivity devices.
Average cross sections obtained from the super cell calculations are
then used in the overall core model as incremental values to apply to
the normal unit cell cross sections.

Typical values for unit cell cross sections are given in
Table 3.2.3-1. These cross-sections are used in the two group diffusion
equations as follows:

$$\nabla \cdot D_2 \nabla \phi - \Sigma_{a,2} \phi + \Sigma_{R,1} \psi = 0$$

$$\nabla \cdot D_1 \nabla \psi - [\Sigma_{a,1} + \Sigma_{R,1}] \psi + \frac{[\nu_2 \Sigma_{f,2} \phi + \nu_1 \Sigma_{f,1} \psi]}{\lambda} = 0$$

where λ is the eigenvalue, ϕ and ψ are, respectively, the thermal and
fast flux. $\Sigma_{R,1}$ is the removal cross section from group 1 to 2.

Table 3.2.3-1 - Lattice Cross-Sections Versus Neutron Irradiation For Fast And Slow Neutrons

Average Discharge Neutron Irradiation (n/kb)	D_1 Fast Diffusion Coefficient (cm)	D_2 Slow Diffusion (x10^{-3}) (cm)	$\Sigma_{a,1}$ Fast Absorption (x10^{-2}) (cm^{-1})	$\Sigma_{a,2}$ Slow Absorption (x10^{-2}) (cm^{-1})	$\nu_2 \Sigma_{f,2}$ Production (x10^{-2}) (cm^{-1})	$\Sigma_{R,1}$ Moderation (x10^{-2}) (cm^{-1})
0	1.274	0.93657	0.76709	0.36895	0.43844	0.74113
0.2	"	0.93661	0.76682	0.37283	0.44222	0.74115
0.4	"	0.93671	0.76655	0.37889	0.45063	0.74118
0.6	"	0.93677	0.76628	0.38399	0.45644	0.74121
0.8	"	0.93681	0.76600	0.38813	0.46000	0.74124
1.0	"	0.93683	0.76573	0.39149	0.46188	0.74129
1.2	"	0.93684	0.76545	0.39424	0.46253	0.74129
1.4	"	0.93683	0.76518	0.39650	0.46228	0.74132
1.6	"	0.93682	0.76491	0.39838	0.46137	0.74135
1.8	"	0.93680	0.76463	0.39996	0.46000	0.74137

In the four-factor formulation used by POWDERPUFS-V, the fast fission rate is not calculated explicitly but relative to the thermal process only. Thus the production of fast neutrons per thermal neutron absorption is given as $\varepsilon\eta f$. The source term for the fast group equation (second equation) therefore reduces to

$$\frac{\nu_2 \Sigma_{f,2}\, \phi}{\lambda}$$

where

$$\nu_2 \Sigma_{f,2} = \Sigma_{a,2} \quad \varepsilon\eta f = \Sigma_{a,2}\frac{k_\infty}{p}$$

The fast group cross sections, $\Sigma_{a,1}$ and $\Sigma_{R,1}$, can be determined from the following relations:

$$\Sigma_{a,1} + \Sigma_{R,1} = \frac{D_1}{L_s^2} \qquad \text{(Diffusion theory)}$$

$$\frac{\Sigma_{R,1}}{\Sigma_{a,1} + \Sigma_{R,1}} = p \qquad \text{(Definition)}$$

giving

$$\Sigma_{R,1} = p\,\frac{D_1}{L_s^2}$$

and

$$\Sigma_{a,1} = (1-p)\,\frac{D_1}{L_s^2}$$

In summary, the two-group diffusion parameters for the lattice cell appropriate to this formulation are calculated according to:

$$\Sigma_{a,2} = \frac{D_2}{L^2}$$

$$\Sigma_{a,1} = (1-p)\,\frac{D_1}{L_s^2}$$

$$\nu_2 \Sigma_{f,2} = \frac{k_\infty}{p}\,\Sigma_{a,2}$$

$$\Sigma_{R,1} = p\,\frac{D_1}{L_s^2}$$

where

$$D_1 = \frac{1}{3 < \Sigma_{tr,1} > cell}$$

and

$$D_2 = \frac{1}{3 < \Sigma_{tr,2} > cell}$$

All quantities on the right hand side are known.

In a reactor simulation, it is usually necessary to simulate the reflector region as well. The two group diffusion parameters for the reflector region are calculated by simple recipes:

$$\Sigma_{a,2,R} = \hat{\Sigma}_{a, moderator} \div \frac{\pi T_o}{4 T_M} = \Sigma_{a,2, moderator}$$

$$\Sigma_{R,1,R} = \frac{D_{1,R}}{L^2_{s,R}}$$

$$D_{2,R} = \frac{1}{3 \Sigma_{tr,2,R}}$$

and

$$D_{1,R} = \frac{L^2_{s,R}}{8.66}$$

where

$$\Sigma_{tr,2,R} = \Sigma_{tr,2, Moderator}$$

and

$$L^2_{s,R} = 126 - 4(100-AP \frac{\rho^2_R (T_o)}{\rho^2_R (T_R)})$$

AP is the purity of the reflector in atom percent. In the program, the physical properties (density, temperature and purity) of the reflector are assumed same as that given for the moderator.

A typical model used for the 3-dimensional core simulation is shown in Figures 3.2-21, 3.2-22 and 3.2-23. A typical model used for the supercell calculation of an interstitial absorber is shown in Figures 3.2-24 and 3.2-25. The former is a schematic and the latter shows the mesh definitions. All reactivity devices and flux detector assemblies in CANDU cores are perpendicular to the fuel channels. However because of the well thermalized spectrum in the CANDU core we find that even the supercell calculations can be done basically in two groups with appropriate boundary conditions applied at the surface of the fuel cell and the absorber cell. Experimental data done at the research reactors at CRNL indicate that comparable agreement is obtained in simulating absorbers in this manner whether they are parallel or perpendicular to the fuel channels.

The models used for the core design analysis are validated by comparison against experimental information. Some of these comparisons were reported by Critoph[1]. Additional information of this type is given in the section on commissioning later in this document.

3.2.3.2.2 Locating In-Core Devices

Adjuster Rods: Establishing the desirable locations for the adjuster rods and finalizing the neutron absorbing characteristics of each rod normally requires a significant number of iterations looking at various possibilities. We have a computer program which can automatically allocate the distribution of absorbing material in a region of the core to achieve certain input objectives. This program greatly reduces the manual effort required in finding an optimum distribution of absorber rods.

A prime function of the adjuster rod system is to make it possible to restart the reactor shortly after a shutdown. When the reactor shuts down or the power level is reduced significantly there is a transient increase in the concentration of ^{135}Xe in the fuel because of the relatively high concentration of its precursor ^{135}I which exists

under steady state full power conditions. The adjuster rods are
provided to permit restarting the reactor, usually within about one half
hour after shutdown, by withdrawing the adjuster rods to compensate for
the increase in ^{135}Xe concentration that has occurred. The effect on
system reactivity due to the increase in ^{135}Xe must be calculated in
order to determine how much absorbing material must be provided in the
adjuster rod system. These calculations are initially done using the
"point-model" approach in which the flux level in the reactor is charac-
terized by a single "effective" value. They are later confirmed with
three dimensional simulations. Calculations of this type reveal that
the adjuster rod reactivity worth needs to be about 14 mk to compensate
for the build-up of ^{135}Xe in 30 minutes following a reactor shutdown.

Comparisons of measured and calculated reactivity worth
values for Pickering and RAPS-1 adjuster rods is shown in Table 3.2.3-2.

Zone Control Absorbers: When the number of fuel channels
and the number and layout of adjuster rods are established the next step
is normally to determine the locations for the liquid zone control
devices. Since daily fuelling of the reactor keeps the fuel burnup
characteristics in the core roughly constant on average and since the
adjuster rods are provided to compensate for transient xenon effects to
the degree deemed necessary, the reactivity range capability of the
liquid zone control system does not need to be very large. Experience
has shown that a total range from empty to full of 5 to 7 mk is adequate.
This is sufficient to compensate for the reactivity decrease due to fuel
burnup that occurs between fuelling operations and in fact permits
several days of operation without fuelling. In a spatial sense it is
also adequate to compensate for the replacement of burned up fuel in a
channel with un-irradiated fuel.

The positions of the zone controllers are largely dictated
by their spatial control function. If the CANDU reactor were not
spatially controlled, unstable oscillations in reactor power distribution

of the first azimuthal type would tend to develop because of spatial variations of ^{135}Xe that would result following a localized flux disturbance. The positions of the zone controllers are initially chosen on the basis of past experience and examining the shapes of the higher harmonics of the flux distributions. We have a computer program which, for any given fundamental steady-state flux shape, produces the corresponding flux distributions for the higher harmonics of the solution of the diffusion equations. When tentative locations are selected a simulation model is set up to determine the effect on the steady state power distribution of the zone control levels being set at their nominal operating point and also to check that the number of sites selected and the dimensions of the tubes containing the H_2O are such as to provide the necessary reactivity range for the system.

The zone control rods are modelled in a matter similar to the other devices such as adjuster rods by performing supercell calculations for those localized regions and deriving incremental cross sections to use in those regions in the core model which has a coarser mesh than the supercell. Comparisons of measured and calculated reactivity worths for the zone controller rods in Pickering A and Bruce A are shown in Table 3.2.3-3.

Shut-off Rod Absorbers: The next step in establishing the core design characteristics is to determine the location and number of the shutoff rods. As mentioned in Section 2 these devices are cylindrical rods of cadmium sandwiched between two steel cylinders with the cadmium thickness chosen to make the rods virtually black to thermal neutrons. None of these rods are in the reactor during normal operation. Therefore, the number and layout are determined solely on the basis of their capability to shutdown the reactor adequately when various postulated accidents occur. The accident which tends to set the performance requirements of the shutoff rod system is the loss of coolant accident.

A major rupture in the primary heat transport system which causes the coolant to discharge very quickly is highly improbable. It is assumed to occur for purposes of designing the shutdown systems since losing the coolant from the fuel channels increases reactivity slightly, as mentioned earlier, and this occurs in a few seconds in the postualted worst case. The speed of insertion of the shut-off rod system and the reactivity worth of the system is dictated largely by this event. The other assumption that is made in designing the shutoff rod system is that any two rods are assumed to be unavailable. Consequently, part of the analysis process is to determine which two rods being unavailable would most affect the performance of the system.

It is typically found that a shutdown system which has approximately 50 mk worth when calculated with the steady state diffusion code calculation gives adequate performance. The tentative design is set on the basis of simulations with diffusion codes of various arrrangement rods. The modelling of the rods is done using a supercell approach to derive incremental properties. The boundary conditions used in the supercell calculation are, of course, different in this case as the rods are much blacker to neutrons than are the adjuster rods or the liquid zone control rods. A further complication is introduced in that fast neutrons do go through the rod and become moderated in the heavy water inside the rod and are then captured. Although this effect is not a large component, it is normally accounted for in the calculations. Comparison of the measured and calculated shutoff rod reactivity rod for the Pickering and Bruce A reactors are shown in Tables 3.2.3-4 and 3.2.3-5. Comparison of the flux distribution measured by copper wire activation when 28 of the 30 Bruce A shutoff rods are fully inserted in the core with the reactor critical is shown in Figure 3.2-26. Note that in this case the two rods assumed to be missing are on the right hand side so the reactivity of the system is largely dictated by that region. The fact that two-group diffusion code calculations give such good agreement in spite of the steep gradients in the flux is considered to be a demanding validation of the core modelling methodology used.

Mechanical Control Absorbers: Another step in the core design analysis is the selection of the positions and numbers for the mechanical control absorbers. These rods physically are the same as shutoff rods but are part of the regulating system. However, during normal operation they are fully withdrawn so their positions are not dictated by the impact they have on the power distribution to any significant degree. The design requirement for these rods is set largely by the need for them to compensate the gain in reactivity associated with reducing power to near zero. For partial setback functions (one or two rods) it is important to assess the power limitations that would be associated with such configurations. Figure C6 in Critoph's lectures[1] shows a comparison of the flux distribution for such a case. Comparison of measured and calculated reactivity worths for these rods in Bruce-A is shown in Table 3.2.3-5.

Poison Injection Nozzles: The location of the poison injection nozzles for the second shut-down system is also determined in the reactor physics analysis associated with the core design. These nozzles are made of zircaloy but have quite a heavy wall so their presence does have a small effect on power distribution and needs to be accounted for in establishing the final reference power distribution for design purposes. These nozzles are horizontally oriented and are perpendicular to all the other reactivity control devices. Their locations are dictated primarily by the dynamics of poison injection which will be dealt with in the next Section.

Flux Detectors: The distribution of flux detectors is normally examined after the other devices have been finalized. They affect power distribution only slightly so their positions are set by the way they are used. This is discussed in the next Section.

Fixed Guide Tubes: Although the shutoff rods and the
mechanical control absorbers are not in the reactor during operation they
each have a guide tube which is a fixed in-core reactor structure made
of zircaloy. Also, there is other hardware at the inside edge of the
calandria to permit positioning these guide tubes and to attach them to
the calandria. The effect of these devices, although small, is examined
in the establishment of the final discharge burnup pattern to recommend
for the operation of the reactor. Therefore, the final modelling of the
reactor core does not include allowance for all the incore hardware.
Use of relatively large mesh spacings gives good accuracy for CANDU
cores because of the large migration length of the lattice. This,
combined with application of the "super cell" method to treat in-core
devices makes it feasible to simulate all this hardware explicitly
without prohibitive expense. A typical calculation of a 3-dimensional
flux distribution in the reactor takes _ 200 seconds on the CDC 6600
(16,000 mesh point model).

TABLE 3.2.3-2

MEASURED AND CALCULATED REACTIVITY WORTH OF RAPS ADJUSTER RODS

	Adjuster Rod Worth (milli-k)
Measured	12.34
Calculated	12.7

MEASURED AND CALCULATED REACTIVITY WORTH OF PICKERING COBALT ADJUSTER RODS

	Total Worth of 18 Adjuster Rods (milli-k)
Unit 1 (Measured)	20.33
Unit 2 (Measured)	18.29
Unit 4 (Measured)	20.09
Mean Worth (Measured)	19.57
Calculated Worth	19.58

TABLE 3.2.3-3

MEASURED AND CALCULATED REACTIVITY WORTHS
OF ZONE CONTROL RODS IN PICKERING 'A'

Pickering 'A'	Moderator Height (m)	Moderator Temperature ($^{\circ}$C)	Total Reactivity Worth of H_2O (milli-k)
Unit 1	7.50	45	4.89
Unit 2	7.28	32	4.89
Unit 3	6.06	39	5.51
Measured value Interpolated at 7.05 m Moderator Height	7.05		5.08
Calculated	7.05	58	4.78
Calculated	7.05	32	4.80

TABLE 3.2.3-4

MEASURED AND CALCULATED REACTIVITY WORTH
OF PICKERING SHUTOFF RODS

	Sum of Single Shutoff Rod Reactivities (milli-k)
Unit 1 (Measured)	27.89
Unit 2 (Measured)	23.69
Unit 4 (Measured	26.40
Mean Worth (Measured)	25.99
Calculated Worth	24.89

TABLE 3.2.3-5

MEASURED AND CALCULATED DATA RELATING TO BRUCE SHUTOFF RODS

BORON EQUIVALENCE

Configuration	Boron Equivalence (mg/kg)		Deviation (percent)
	Calculated	Experimental	
30 shutoff rods	3.45	3.30	+4.5
28 shutoff rods	2.75	2.65	+3.8

REACTIVITY WORTH (Individual or Small Groups of Rods)

Configuration	Reactivity Worth (milli-k)		Deviation (percent)
	Calculated	Experimental	
Shutoff rod 5	1.51	1.41	+7.1
Shutoff rod 20	1.46	1.49	2.0
*Mechanical control rods 3 and 4	2.59	2.53	+2.4
*Mechanical control rods 1, 2, 3 and 4	4.96	4.80	+3.3

*These rods are physically identical to shutoff rods, but are used for control purposes only.

3.2.4   Time Dependent Analyses

Once the basic reference design of the reactor core is established based on "static" simulations with 3-dimensional two-group diffusion codes, as discussed previously, it is necessary to verify the dynamic performance of the regulating and protective systems. Time dependent phenomenon which need to be studied fall into three general time domains:

(a)   The day to day refuelling of the reactor must be simulated during the design phase to a sufficient degree to assess the discrete effects associated with the fact that fuelling is in reality not continuous but is done by replacing small batches of fuel at a time. The reference fuelling scheme for the CANDU-600 calls for replacing 8 fuel bundles within a channel upon each visit to a fuel channel. Also because of fuel scheduling restraints several channels may be fuelled within a relatively short interval of time and then no fuelling done for a longer period. These effects cause localized distortions in the power distribution relative to that calculated with the reaction rate averaged model that was described previously. These aspects will be discussed in detail in the lectures on fuel management later in this course.

(b)   Transient trends in ^{135}Xe concentration occur in the time domain of hours rather than days and these effects are treated by a different computer program than used for fuel management simulations.

(c)   The time response of the shutdown systems following an assumed accident results in gross change in the reactor flux distribution in the time scale of seconds. This again is a different class of problem

as delayed neutrons have a substantial impact on the
flux shape. We will discuss in some detail the
methods used to treat the xenon problem and the
reactor shutdown transient problem in the following.

3.2.4.1   Xenon Transients

The ability to simulate space and time variation of ^{135}Xe
concentration in the reactor is important for two main reasons:

(1)   to verify that the liquid zone control system can
adequately control the power distribution following
localized disturbances that can occur during normal
operation such as refuelling channels. Spatial
variation of ^{135}Xe in response to a local distur-
bance is the main reason a spatial control system is
provided.

(2)   The xenon transient following a reduction in reactor
power does vary spatially as the ^{135}I precursor
distribution is proportional to the flux distribu-
tion in the steady state full power operating mode.

A computer program has been developed to permit calcula-
tion of the xenon distribution in the reactor in space and time and
simultaneously calculates the corresponding effect on power distribution
and overall reactivity. This program is based on the two-group diffusion
equations, but the equations describing the xenon and iodine variation
as a function of the local flux are also included. The code is "quasi-
dynamic" in the sense that transients are simulated as a series of
steady state cases with the flux assumed constant over a time interval
but then updated in the next interval. The program also includes
capability to simulate the response of the liquid zone control system to
re-distribution of the xenon and iodine or in response to other localized
perturbations.

The algorithm used in the spatial control system of the reactor which couples changes in local or regional flux and/or power to response of the individual zone controller compartments is put into the program, at least in an approximate way. The time steps used in the program are consistent with the time variation of the xenon concentration so the program is geared specifically to verify that the control system can prevent uncontrolled oscillations being induced by xenon feed-back effects. It does not explicitly simulate the hydraulic dynamics of the liquid zone control system. Required changes in water levels in individual control compartments are assumed to occur instantaneously.

The performance of the zone control system is typically verified by assuming that various fuel channels are completely refuelled with fresh fuel and observing the response of the zone control system to this disturbance. It is followed in time long enough to be sure that either the new stable condition has been reached or is clearly being approached. Figure 3.2-27 shows typical variation of the side-to-side and top-to-bottom tilt in the reactor following a refuelling disturbance.

Another application of the spatial control simulation computer program is to calculate the performance of the reactor regulating system and to predict accurately the time variation of reactor power distribution following a reduction in reactor power or during recovery from a reactor trip. When the reactor power is quickly set back to some lower level and held there for some time the ^{135}Xe concentration will temporarily increase and then decay to a level slightly lower than the original value. As the xenon concentration increases the liquid zone control system will tend to empty to compensate. Before it reaches the empty condition, the regulating system activates one group of the adjuster rods and they are withdrawn. Since they are driven out steadily until fully out, the zone control system must fill to compensate. The rods are divided into a number of banks selected such that a complete

withdrawal of any one bank can be more than compensated by filling of
the liquid zone control system. (The withdrawal of the adjusters causes
a change in the reactor power distribution so it is important to simulate
that as well with the computer program. This is done by a semi-automatic
process.) As the xenon concentration continues to increase the zone
levels will be allowed to drain again at which time another group of
adjusters will be withdrawn. This process means that the reactor does
not operate for significant periods of time with adjusters partly
inserted and hence partial insertion conditions do not need to be simulated
in detail.

Similarly, it is important to simulate a reactor startup
following a short shutdown. If the reactor has been shutdown to the
time limit allowed by the design of the adjuster rod system, all of the
adjuster rods will have to be withdrawn to restart the reactor and raise
power to a level sufficiently high to turn the xenon transient over.
Therefore, in this case the simulation consists of tracing the power
history and reactivity as xenon burns out and adjuster rods are driven
in one bank at a time. This is necessary to verify that the reactor
power can be raised sufficiently high to turn the xenon transient over
without overrating the fuel due to the peaking effect caused by adjuster
rods being withdrawn. A typical startup power history is shown in
Figure 3.2-28.

3.2.4.2   Shutdown System Performance Analysis

As mentioned previously the loss of coolant accident is
the event that tends to determine the design requirements of the shut-
down systems. In examining the consequences of this event it is impor-
tant to be able to predict the time variation of the power in each fuel
bundle in the reactor reasonably accurately. In the CANDU-600 the
primary transport system is divided into two circuits. When one of
these circuits loses the coolant the channels in one half of the reactor
are voided. Because of the associated small positive reactivity effect,

the power rises somewhat preferentially in that side of the reactor which activates an overpower trip and causes the shutdown system to activate.

In the case of the shutoff rod system, the rods are dropped into the core within about two seconds. Since this time is comparable to the half-life of many of the delayed neutrons precursors it is important in simulating this event to correctly account for the space-time variation of the delayed neutron precursors. When the power decreases their relative contribution to the overall neutron balance becomes increasingly important. A computer program has been developed to permit this type of calculation to be done. It is a 3-dimensional code which employs the improved quasi static approximation (IQS)[14][15]. In this method the space and time dependent flux is factored into an amplitude function which is only time dependent and a space function which is only weakly depending on time.

The IQS method is a flux factorized method developed to solve the time-dependent multigroup diffusion equation;

$$[-M + F_p] \phi (r,E,t) + S_d[\phi(r,E,t')] = \frac{1}{v} \frac{\partial}{\partial t} \phi (r,E,t)$$

where M is the removal and scattering operator, F_p the prompt fission source operator, and S_d the delayed neutron source. The total flux is factorized into an "amplitude" function $\phi(t)$ and a "shape" function $\Psi(r,E,t)$:

$$\phi(r,E,t) = \phi(t) \, \Psi(r,E,t) \qquad (\phi(o) = 1.0)$$

with the condition that $\Psi(r,E,t)$ is only weakly dependent on time and hence ϕ and Ψ are uniquely defined. This constraint is satisfied by forcing the integral

$$\iint \frac{\Psi^*(r,E,o) \, \Psi (r,E,t)}{v} \, dr \, dE$$

to be constant. With this condition the amplitude equation for $\phi(t)$ reduces to the point kinetics equation:

$$\frac{d\emptyset(t)}{dt} = \frac{[\rho(t) - \beta(t)]}{\Lambda(t)} \; \emptyset(t) + \Sigma \; \lambda_k \; C_k \; (t)$$

where the integral quantities $\rho(t)$, $\bar{\beta}(t)$, etc. must be derived by suitable averaging with the time dependent shape function $\Psi(r,E,t)$.

Upon substitution of the factorized total flux into the diffusion equation the shape equation takes the form:

$$[-M + F_p] \; \Psi(r,E,t) + \frac{S_d[\emptyset(t') \cdot \Psi(r,E,t')]}{\emptyset(t)}$$

$$= \frac{1}{v} \; [\frac{d\emptyset}{dt} \cdot \frac{\Psi(r,E,t)}{\emptyset(t)} + \frac{\partial}{\partial t} \Psi(r,E,t)]$$

The unique approach in the IQS method is to replace the deriative $\frac{\partial}{\partial t} \Psi(r,E,t)$ by a backward difference of first order:

$$\frac{\partial}{\partial t} \Psi(r,E,t) = \frac{[\Psi(r,E,t) - \Psi(r,E,t - \Delta t)]}{\Delta t}$$

This approximation is valid when $\Psi(r,E,t)$ changes slowly, compared to $\emptyset(t)$. It then allows larger Δt intervals and the integral constraint condition is automatically satisfied within the interval Δt.

For a more detailed discussion of the IQS method the reader is referred to the paper by Kugler and Dastur[15].

The space function is calculated in 3-dimensions, two energy groups, using a variable X-Y-Z mesh. Generally six delayed neutron precursor groups are used although more groups (to accommodate photo-neutrons explicitly) may be used. The code can simulate accurately flux shape retardation effects due to delayed neutron "hold-back" following an asymmetric coolant voiding, shutdown system action, etc. Point kinetics codes are used to analyse situations where spatial effects are not important or may be used to do parametric studies involving small changes in variables relative to a case which has been done with the complete 3-dimensional approach. This code is used to simulate both

shutoff rod performance and performance of the liquid injection shutdown system. Comparison of this method against the experimental results in Bruce A are discussed in Section 4.

The simulation of the performance of the poison injection shutdown system is a particularly challenging analytical task, as the geometrical characterization of the poison as a function of time after activation of the system is difficult. This is because it is very difficult to analytically determine the characteristics of the jets of poison penetrating into the moderator from each of the small holes in the poison injection nozzle. It was necessary, therefore, to empirically determine the characteristics through tests. These tests consisted of mocking-up one of the poison injection nozzles in a tank of water and using a colored solution to represent the gadolinium solution being injected into the moderator under high pressure. By photographing the nozzle from different angles with high-speed cameras the behaviour of the poison could be fairly well determined. Figure 3.2-29 shows what was observed schematically. Typical modelling of the system for purposes of simulating the neutronic behaviour is shown in Figure 3.2-30.

Although the modelling does represent significant approxi-mations, the calculated power transient following activation of this system in the Bruce A reactor during commissioning agreed quite well with the experimental data as shown in Figure 3.2-31. The curve labelled "fast transient" is the best estimate with no conservatisms built in. The "slow transient" calculation has conservative input and is used in safety analysis. Note that the agreement between prediction and experi-ment is very good during the early part of the transient and then deviates from the experimental data with the calculation giving a slower reduction in the neutron flux with time than the experiment. This is not unexpected as the modelling of the poison injection into the modera-tor beyond the time at which the jets no longer have any geometrical definition is not possible. Therefore, in the model it is assumed the poison does not disperse but rather remains in the jet form. In reality

the poison does disperse which has the effect of reducing the self-shielding of neutrons within the poison and hence enhancing the reactivity effect with time relative to that assumed in the calculation.

3.2.4.3 Modelling of Loss of Coolant Accidents

As mentioned before, the void reactivity effect in the CANDU-PHW is positive. Therefore the initial effect associated with a loss of coolant incident would be a tendency for the power to rise until the shut-down system is called into play. There are three factors which mitigate the power pulse due to a loss of coolant.accident: subdivision of the coolant circuit; a long prompt neutron lifetime; and the magnitude of the delayed neutron fraction due to the photo-neutron contribution.

The primary heat transfer system is divided into two independent figure-of-eight circuits. A schematic of one such circuit is shown in Figure 3.2-32. These circuits are interconnected only via a pressurizer and a purification system. If one circuit suddenly depressurizes due to a break the inter-connect valves are closed, so the LOCA effect is confined to only half the core. Figure 3.2-23 shows the variations of average coolant density with time in the voided circuit for a hypothetical 100% break of the inlet header. This density variation is calculated with a thermohydraulic blow-down code. The density is assumed to take place throughout the fuel channels which are cooled by that circuit. Figure 3.2-33 also shows the reactivity transients (with and without shutdown system action). One second after the break the reactivity would be about 3 mk. However, a shutdown system would be brought into play and would turn over the reactivity transient at about .65 secs. after the break, thereby limiting the maximum reactivity insertion to less than 2.5 mk. The neutronic response to such a reactivity insertion is discussedbelow.

The prompt neutron lifetime in a CANDU lattice is relatively long (.9 milli-sec.) compared to most other reactor designs. In

addition, the delayed neutron fraction is enhanced due to the presence
of delayed photo neutrons (produced by dissociation of deuterons by high
energy gamma rays from fission products). These two factors slow down a
potential power excursion considerably. Figure 3.2-34 shows typical
power pulse for the hottest fuel bundle due to header breaks of different
sizes followed by the action of one of the shutdown systems. The percent
header break size figures shown are based on the percentage of the
theoretical maximum break size resulting from a hypothetical type separa-
tion of the pipe. The peak power is only about a factor of 1.5 above
the operating level and the short term (0→2.5 s) power pulse is only 2.6
full power seconds. Experimentally it has been found that a heat
content of at least 200 calories per gram is required for spontaneous
fuel breakup. This is equivalent to about 9 full power seconds for the
maximum rated fuel pin. This means that spontaneous fuel breakup is not
a safety concern during LOCA in the CANDU-PHW.

Since the difference in the neutron lifetime in the CANDU
reactors, relative to light water reactors, are quite significant in
respect to modelling of fast neutronic transients in the core, we will
discuss this aspect in some detail.

The influence of a longer prompt neutron lifetime on a
power excursion is illustrated more clearly in Figures 3.2-25 and
3.2-26. These figures show two hypothetical reactivity transients and
their associated power pulses with different values of ℓ^* (prompt neutron
lifetime). Reactivity transient 1 roughly corresponds to a LOCA event
followed by a shutdown system action in a 600 MWe CANDU. Transient 2 is
a hypothetical transient with a reactivity insertion almost equal to the
delayed neutron fraction (a condition called prompt critical). Neutron
power transients marked A and B correspond respectively to an ℓ^* value
of 0.9 milli-secs. (characteristics of the CANDU) and a value of 0.03
milli-secs (characteristics of light water reactors). One can see that
for reactivity transients well below prompt critical the effect of
different ℓ^* values is small. However for reactivity insertions at or
near prompt critical the larger ℓ^* retards the power pulse significantly.

For CANDU reactors this is an important consequence since it reduces the demands placed on the shutdown design to relatively modest performance requirements.

The above example illustrates clearly the effect different ℓ^* values on the power excursion. Fuel temperature feedback effects should be considered in a realistic evaluation of accidental excursions. The simulation of a LOCA and a consequent activation of a shutdown system is simulated as mentioned before with a 3-dimensional quasi-static method. This method is also applied to simulate the shutdown system tests that are done during commissioning of the nature described previously. We find it important to account properly for the spatial variation of delayed neutrons with time during the insertion of the shutoff rods to properly predict the variation of neutron flux with time.

The importance of the delayed neutron precursor distribution on the flux shape during a shut-off rod insertion transient, and hence on the "effective" reactivity of the shut-off rods at a given time is illustrated in Figure 3.2-37. A parametric study was done of the effect of the speed of insertion of shut-off rods on the dynamic performance of the system for a typical CANDU reactor. The only difference in the two calculations used to produce the curves in this figure is the speed of insertion of the rods. The arrow shown on each curve is the time at which the rods reached the centre-line of the core. Note that although the same amount of absorbing material is in the core at each of these points, the "effective" dynamic reactivity worth of this material is significantly different. Only a small part of that difference is due to the fact that more voiding of the core has occurred in the "slower" case. Most of the difference arises from the fact that in the "faster" case the flux shape is more strongly influenced by the delayed neutron precursor distribution that existed in the core prior to the initiation of the postulated loss-of-coolant and subsequent shut-off rod insertion.

3.2.5   On-Line Flux Mapping

The CANDU-600 is provided with an on-line flux mapping system as part of the regulating system software. This system produces detailed flux and channel power distributions based on in-core self powered vanadium flux detectors. This information is used to provide a calibrated average zonal flux signal for use by the spatial control system, local overpower detection which activates the power setback routine, and on-line power distribution data for reactor operator information. It may also be used as a means of producing current power distribution information for purposes of calibrating the regional over-power protective system. A flux map is typically calculated automatically in approximately two minute intervals.

The task of the reactor physicist in the design of this system is to develop the software for the on-line control computer which can operate on the measured fluxes as indicated by the vanadium detector currents and produce a more comprehensive picture of the flux distribution in the reactor. The power distribution can also be determined from the flux distribution if the fuel burnup characteristics are known.

The techniques of flux mapping consists essentially of a snythesis of the flux distribution from a pre-selected set of flux shape calculations, called flux modes. The amplitudes (i.e. the relative contributions) of the various flux modes are calculated by basically a least squares fitting of relative fluxes measured by vanadium incore flux detectors. The flux modes usually consists of a fundamental mode plus thirteen of the higher harmonics of the flux distribution, plus a set of "perturbation" modes. The latter are flux distributions calcula-ted for a variety of normal operating conditions that may occur such as during periods when the adjusters are not all inserted because they are compensating for transient variation in xenon concentration in the reactor. All these flux shapes or modes are pre-calculated once in an

off-line simulation using the standard two-group diffusion codes that
have been discussed previously. A set of coupling coefficients are
obtained from these simulations as follows:

It is assumed that the thermal flux $\phi(\vec{r})$ at an
arbitrary point r in the core can be expressed as a linear combination
of "realistic" flux shapes ψ_n, described above, i.e.

$$\phi(\vec{r}) = \sum_{j=1}^{5} \alpha_j \psi_j(\vec{r})$$

where $\psi_j(\vec{r})$ is the flux value at $\vec{r}$ when the reactor operates in the
flux mode ψ_j. The above expression is general and is therefore also
valid at detector sites

$$\phi(r_d) = \sum_{j=1}^{5} \alpha_j \psi_j(r_d)$$

Thus, the objective is to obtain the coefficient α_j given the fluxes
$\phi(r_d)$ at the detector locations so they can be used in the first equation
to calculate the flux at points $\vec{r}$ in the reactor.

These coefficients are stored in the normal station
digital control computer. The least squares fitting algorithm involves
essentially one matrix vector multiplication to obtain the mode ampli-
tudes, and a second matrix vector multiplication to obtain an extended
flux map. Approximately 30,000 words of disc storage is required. A
flux map calculation takes about one second of on-line computer time.

The input to the flux mapping system is provided by
outputs from about 100 vanadium self-powered incore detectors. These
detectors are located on 26 vertical flux detector assemblies (as described
in Section 2. The vanadium detectors are calibrated individually prior
to their installation in the reactor so that they accurately reflect the
correct relative flux at their respective locations.

More detailed descriptions of safety related aspects of
the CANDU reactor design are given in a report by G. Kugler[3]. The
flux mapping system is described in more detail by Kugler and Hinchley[16].

OUTPUTS

1 – CROSS SECTIONS VS BURNUP
   – ISOTOPIC COMPOSITION
   – VOID EFFECT (POINT MODEL)
   – REACTIVITY COEFFICIENTS
   – POWER DISTRIBUTION IN FUEL
     BUNDLES, ETC.

2 – CONTROL DEVICES LAYOUT
   – POWER DISTRIBUTION IN THE CORE
   – SHUTDOWN SYSTEMS
   – VOID EFFECT, ETC.

3 – Xe OSCILLATION STUDIES
   – ZONAL OVERPOWERS AND DETECTOR
     LOCATIONS
   – SEQUENCES OF WITHDRAWAL OR
     INSERTION OF CONTROL
     DEVICES, ETC.

4 – POWER PULSE
   – ADEQUACY OF SHUTDOWN
     SYSTEMS, ETC.

5 – FUELLING SCHEMES
   – SIMULATION

◊ INDICATES FEEDBACK
   INFORMATION FROM
   EXPERIMENTAL AND
   POWER REACTORS

REACTOR DESIGN REQUIRE-
MENTS:

– FUEL CHANNEL
– POWER LIMITATIONS
– TEMPS, MATERIALS, ETC.

LATTICE CODES:
– POWDERPUFS
– LATREP
– TRANSPORT CODES

REACTIVITY DEVICE
SIMULATIONS:
– 3-D DIFF. CODES
– 2-D TRANS. CODES

①

CORE DESIGN
CONTROL DEVICES
SHUTDOWN SYSTEMS:
– CHEBY

②

KINETIC STUDIES:
– CERBERUS

FUEL MANAGEMENT
STUDIES:
– FMDP

REACTOR CONTROL
TRANSIENTS DUE
TO PERTURBATIONS/
FLUX MAPPING:
– MONIC
– CHEBXEMAX

④   ⑤   ③

FIGURE 3.1-1   A SIMPLIFIED CHART OF THE PHYSICS ANALYSIS OF PHW REACTORS

FUEL ELEMENT
D₂O COOLANT
PRESSURE TUBE
AIR GAP
CALANDRIA TUBE
D₂O MODERATOR
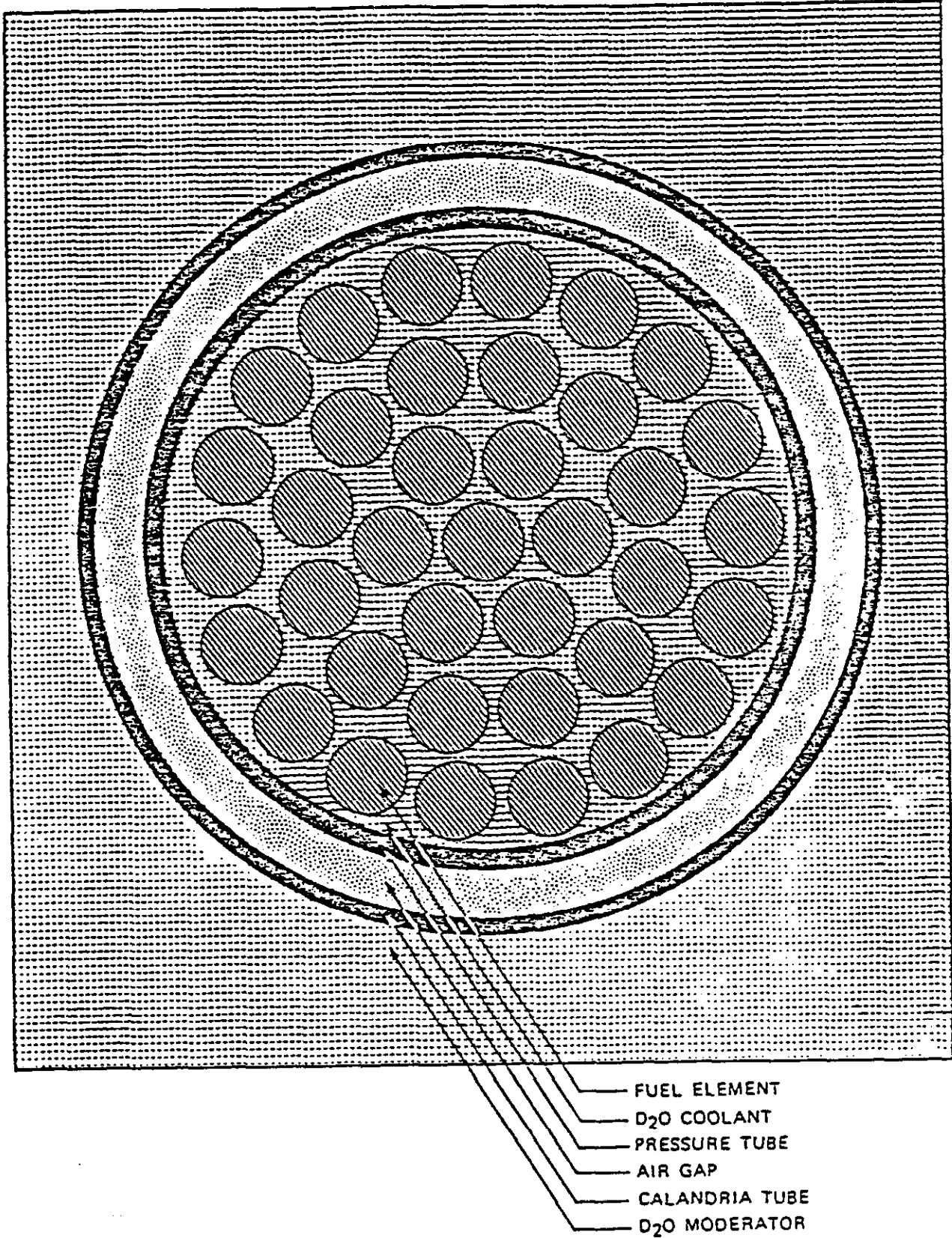
FIGURE 3.2-1   LATTICE CELL FOR 37-ELEMENT FUEL

FIGURE 3.2-2 28-ELEMENT URANIUM OXIDE LATTICE, MATERIAL BUCKLING VERSUS PITCH

MATERIAL BUCKLING (m^{-2})

HEXAGONAL PITCH (cm)

EXP'T   PPV

D$_2$O COOLANT: O ———

AIR COOLANT: X ··········
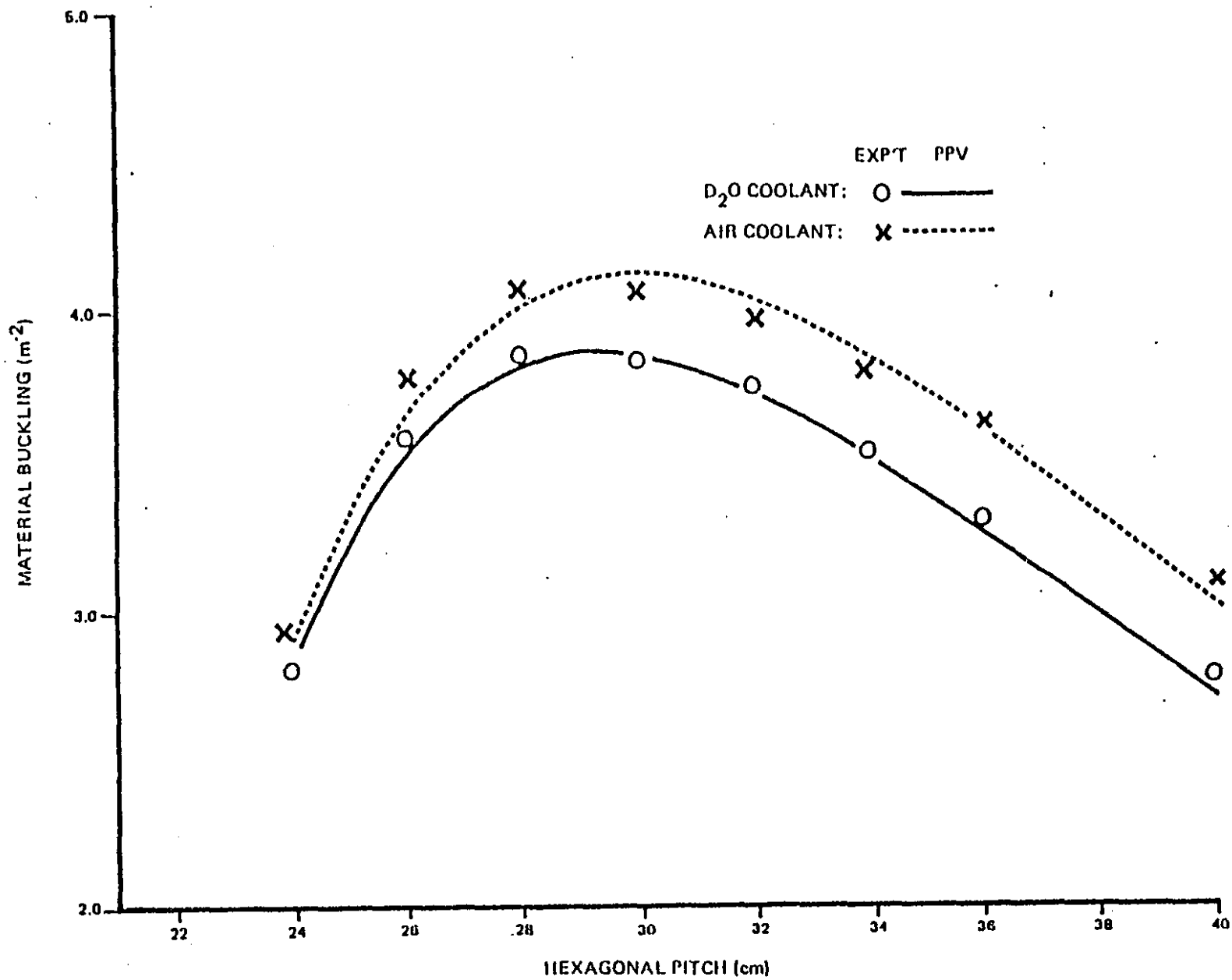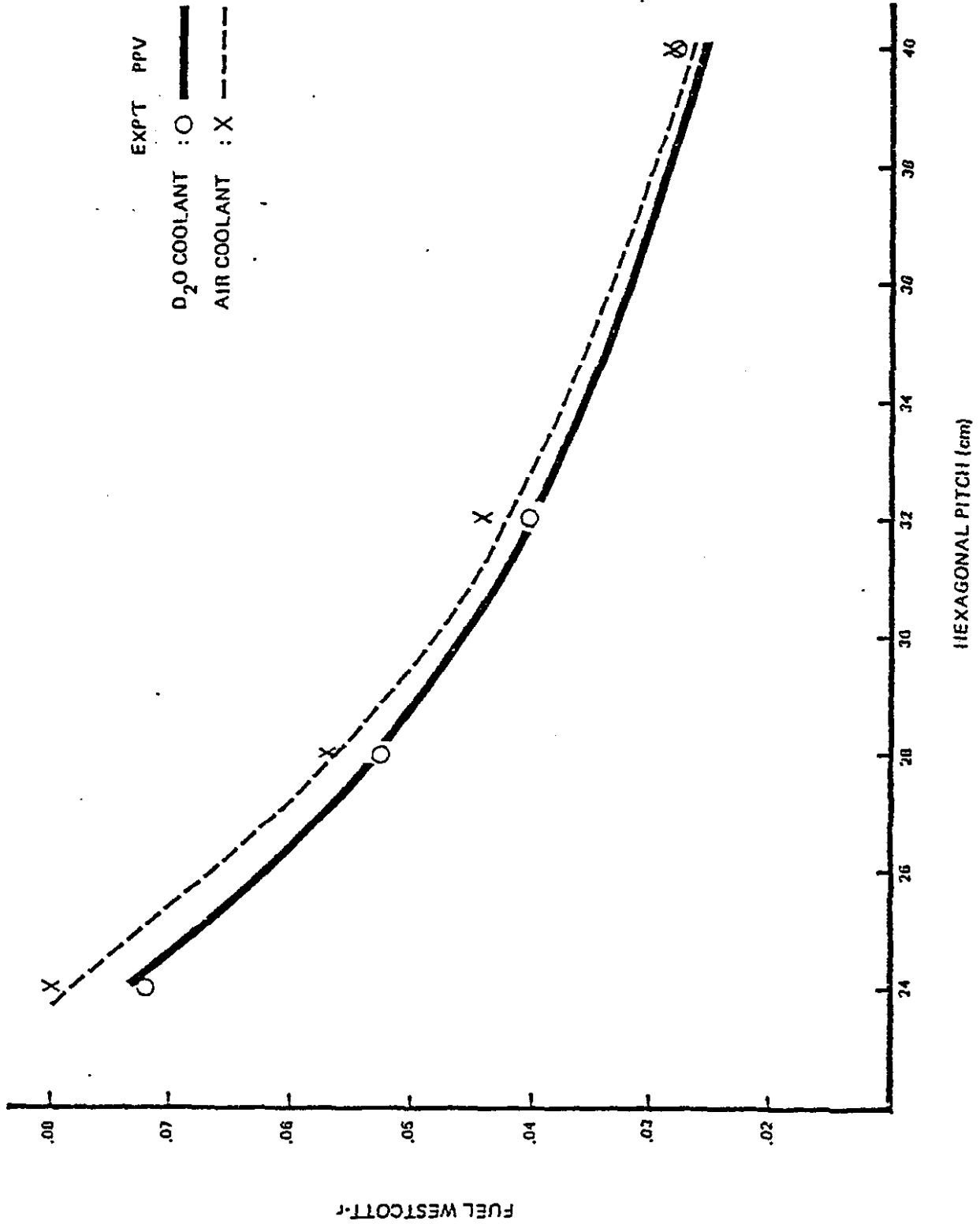
FIGURE 3.2-3 28-ELEMENT URANIUM OXIDE LATTICE, FUEL
WESTCOTT-R VERSUS PITCH
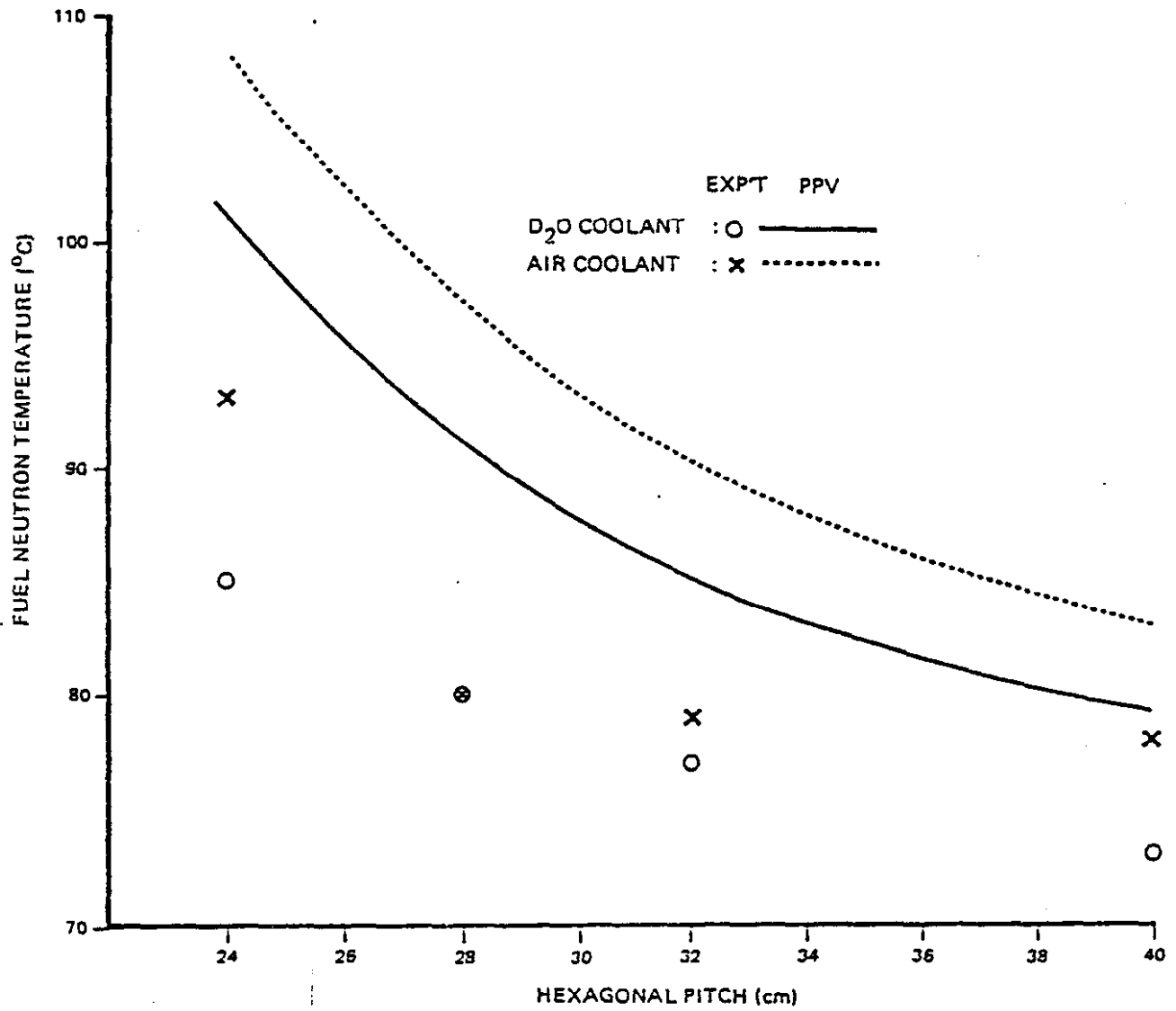
FIGURE 3.2-4   28-ELEMENT URANIUM OXIDE LATTICE, FUEL NEUTRON
TEMPERATURE VERSUS PITCH
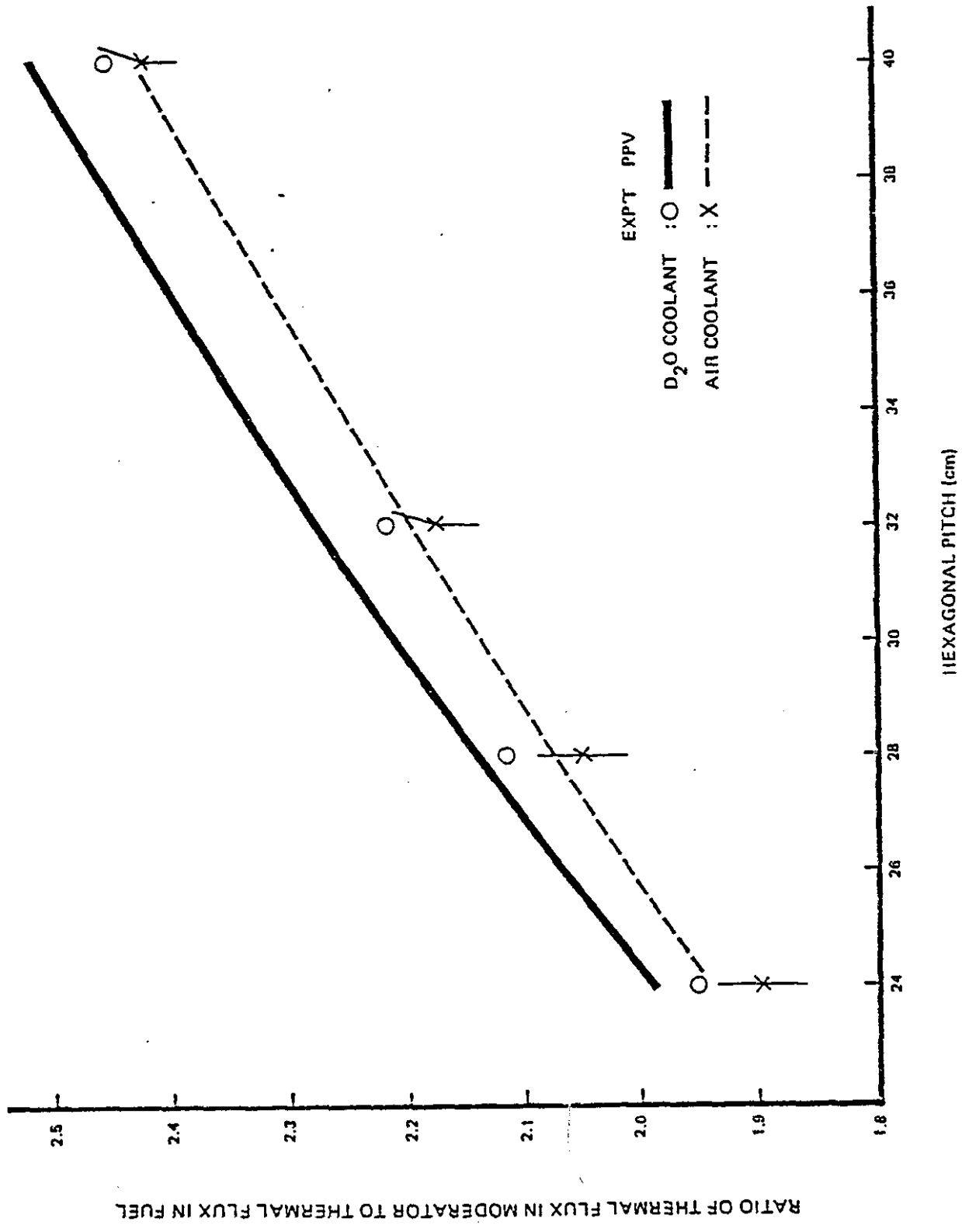
FIGURE 3.2-5 28-ELEMENT URANIUM OXIDE LATTICE RATIO OF
THERMAL FLUX IN MODERATOR TO THERMAL
FLUX IN FUEL VERSUS PITCH
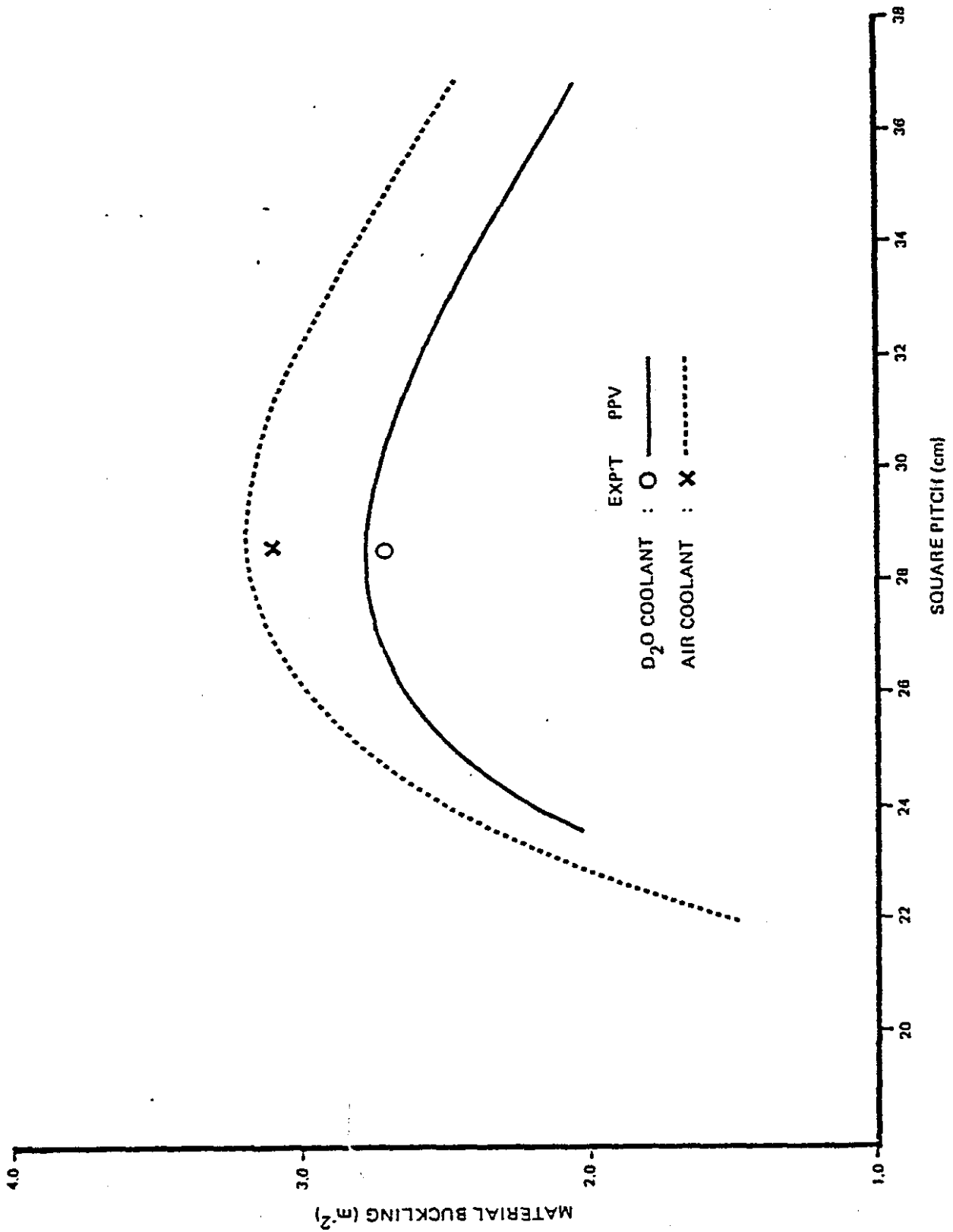
FIGURE 3.2-6   37-ELEMENT URANIUM OXIDE LATTICE,
MATERIAL BUCKLING VERSUS PITCH
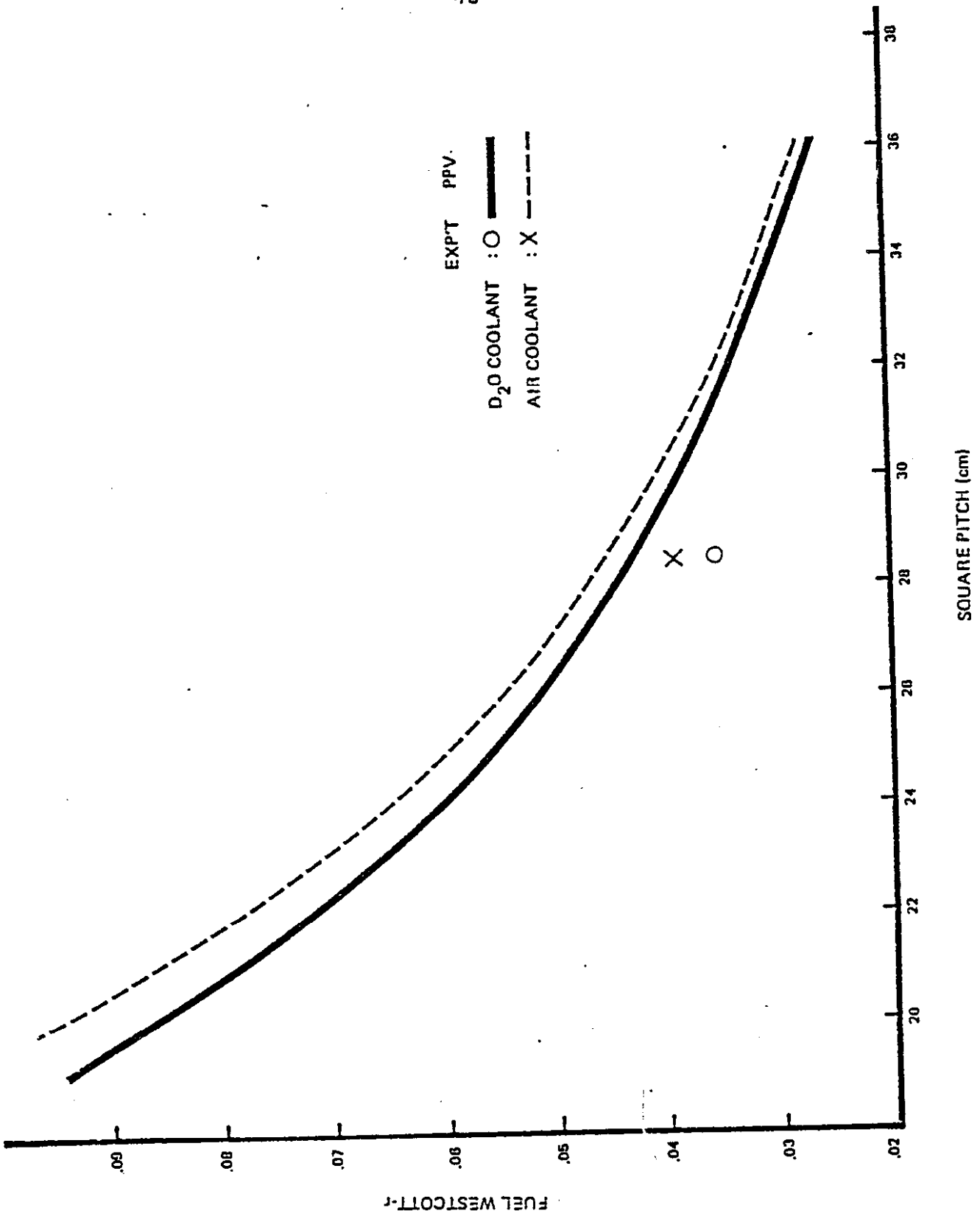
FIGURE 3.2-7   37-ELEMENT URANIUM OXIDE LATTICE, FUEL
WESTCOTT-R VERSUS PITCH
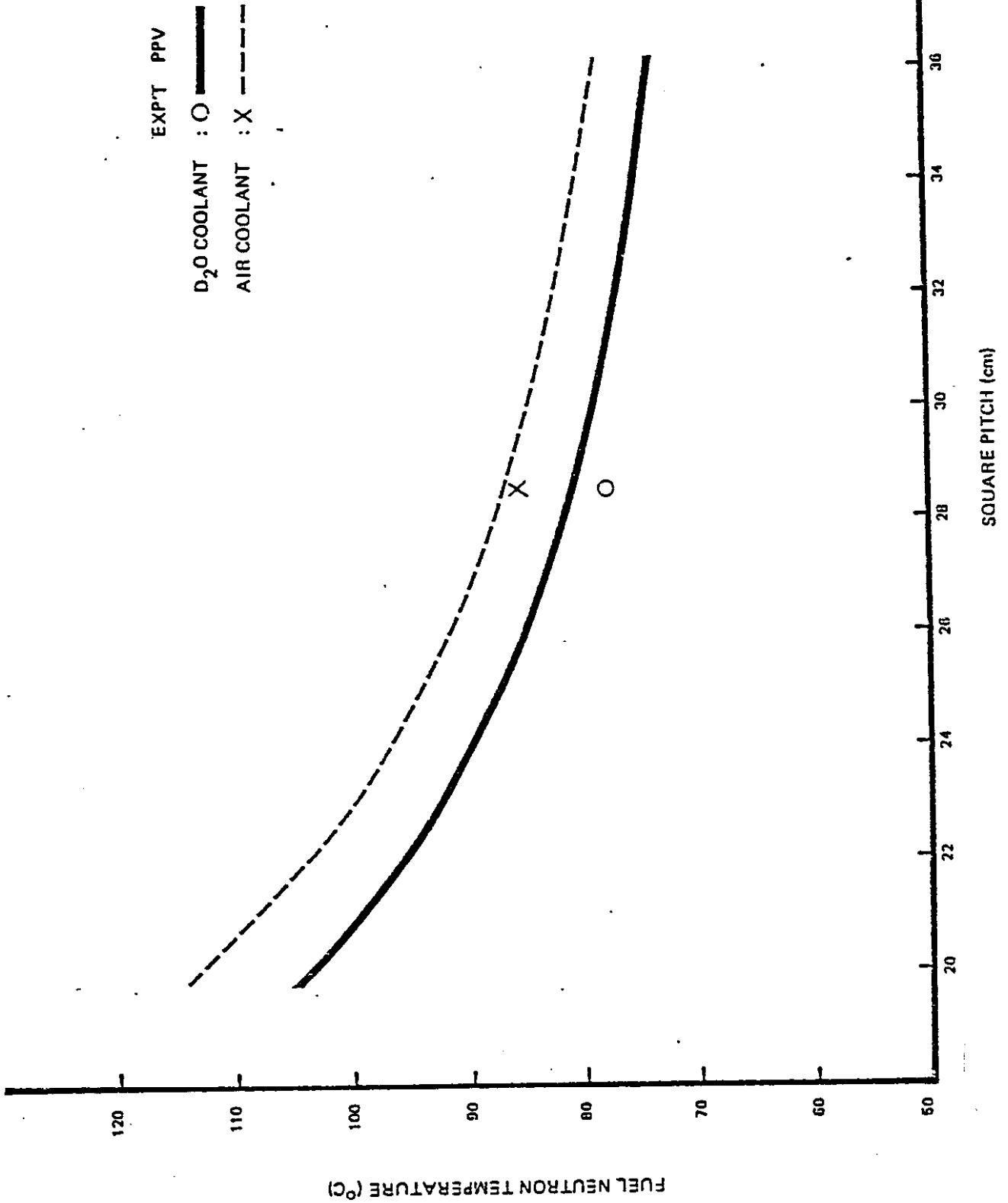
FIGURE 3.2-8 37-ELEMENT URANIUM OXIDE LATTICE, FUEL
NEUTRON TEMPERATURE VERSUS PITCH
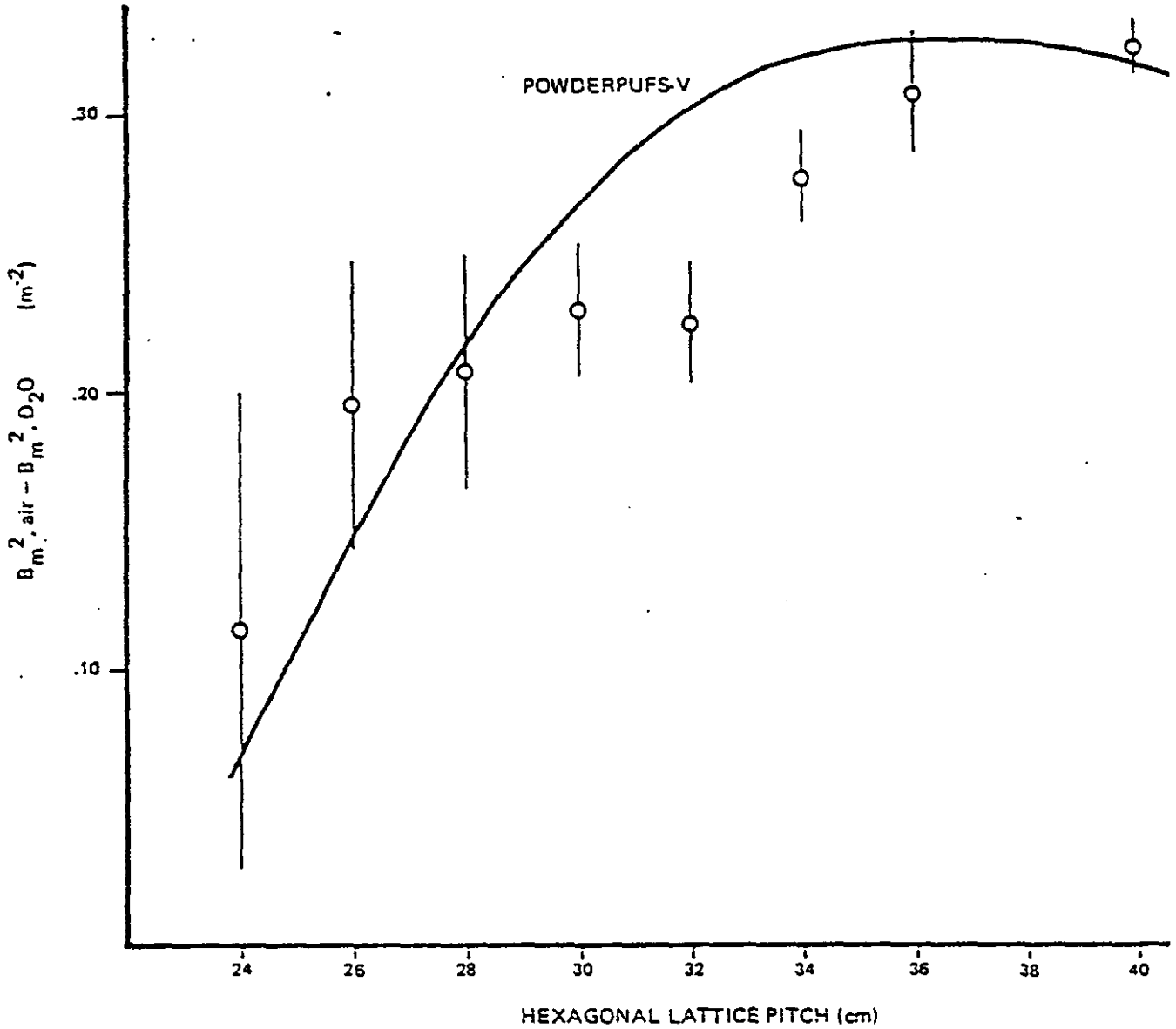
FIGURE 3.2-9   28-ELEMENT URANIUM OXIDE LATTICE, VOID COEFFICIENT
OF MATERIAL BUCKLING VERSUS PITCH
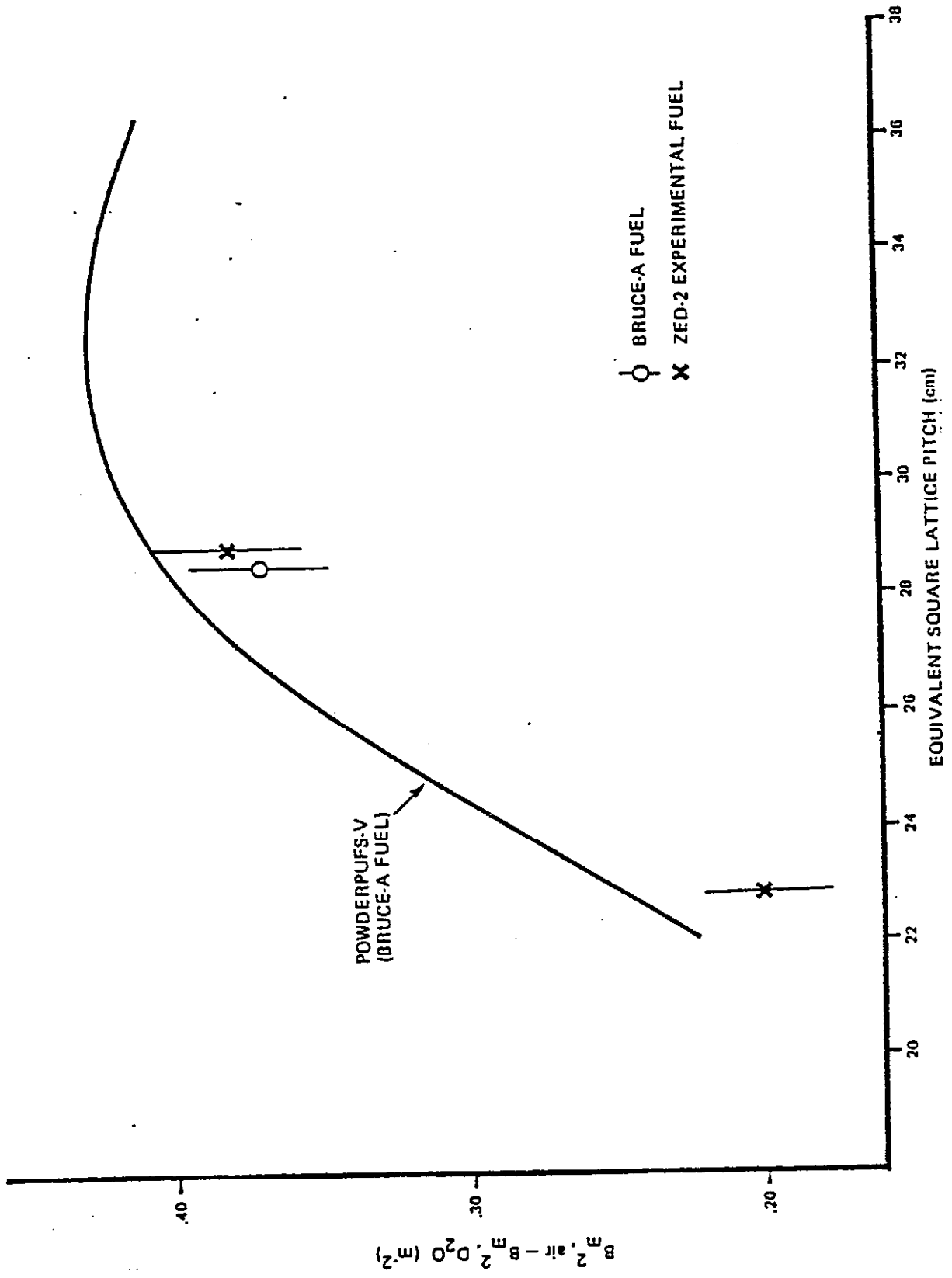
FIGURE 3.2-10   37-ELEMENT URANIUM OXIDE LATTICE, VOID
COEFFICIENT OF MATERIAL BUCKLING VERSUS
PITCH
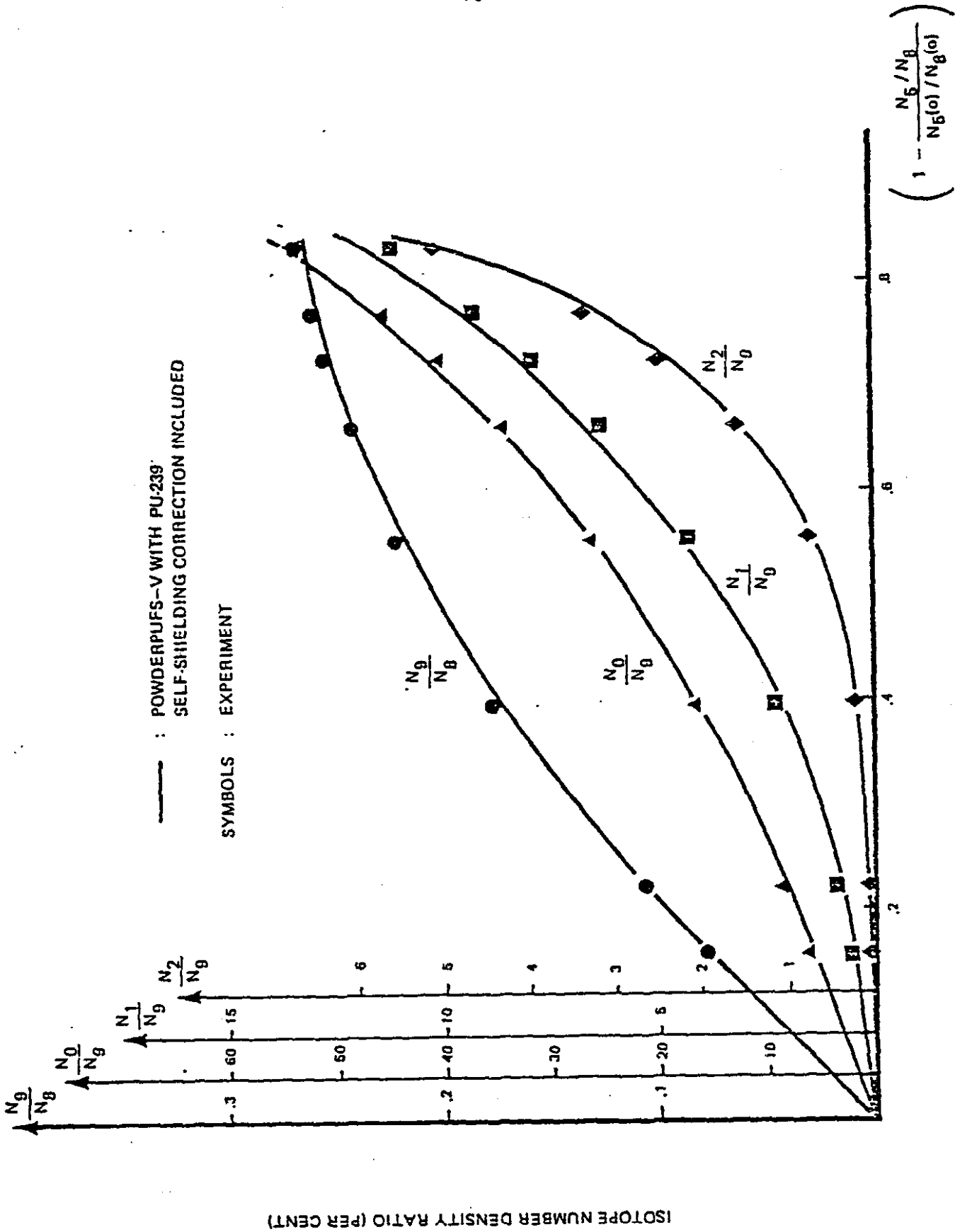
FIGURE 3.2-11   BUNDLE AVERAGE NUCLIDE RATIOS, COMPARISON BETWEEN
MODIFIED POWDERPUFS-V AND EXPERIMENT
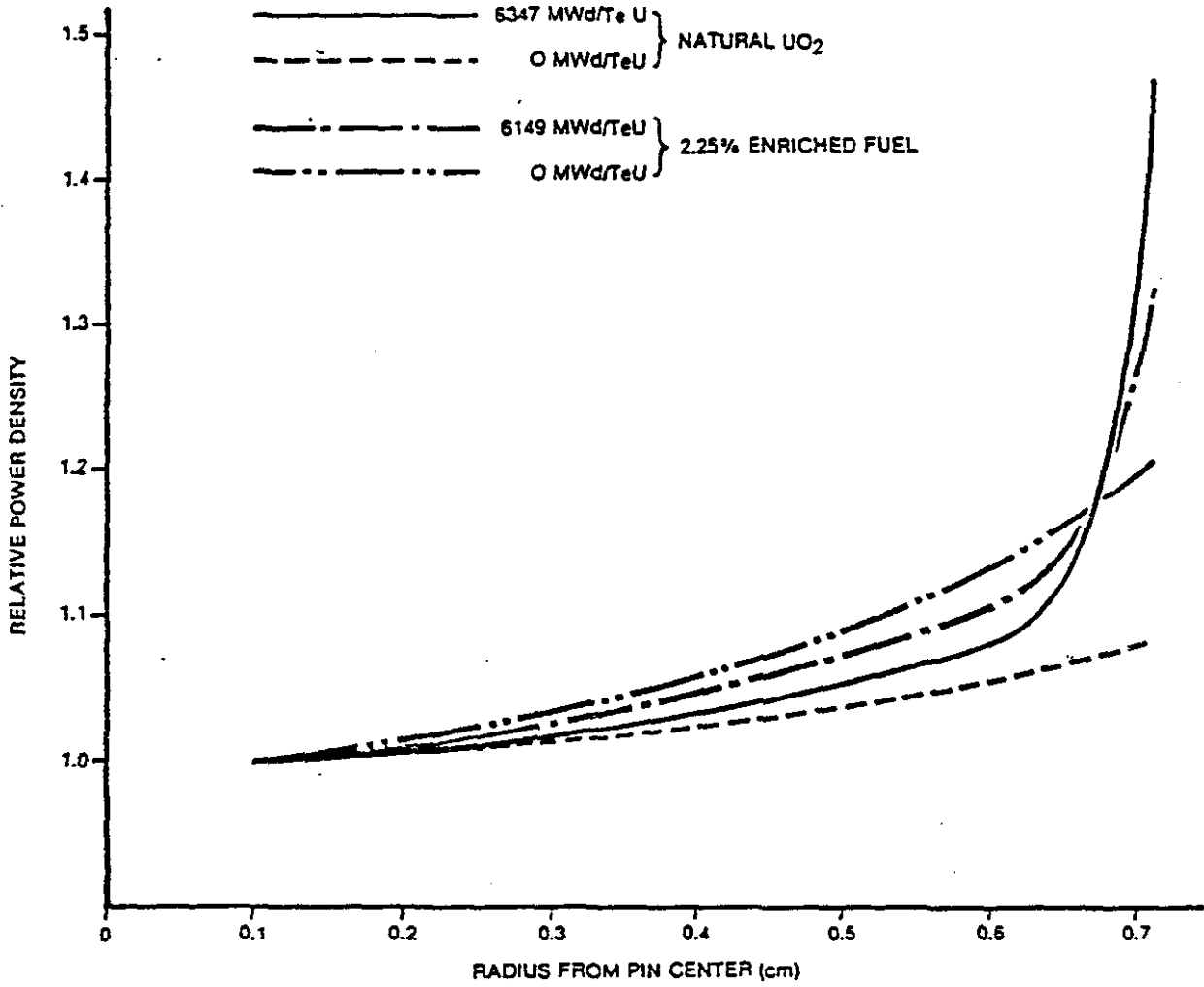
FIGURE 4.2-12 POWER DENSITY DISTRIBUTION IN SINGLE PICKERING UO₂ FUEL PINS

-81-
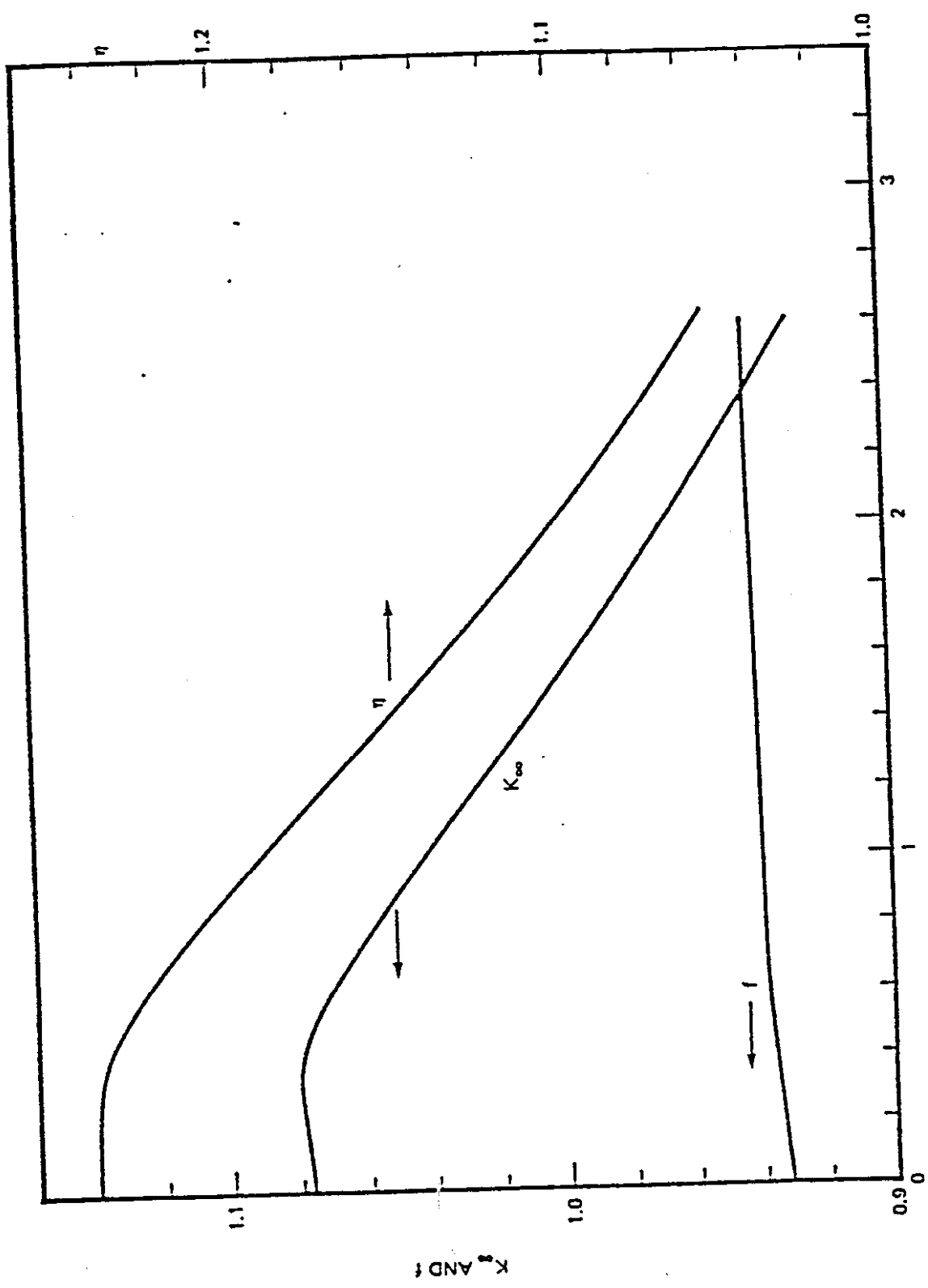
FIGURE 3.2-13 VARIATION OF LATTICE PARAMETERS WITH IRRADIATION
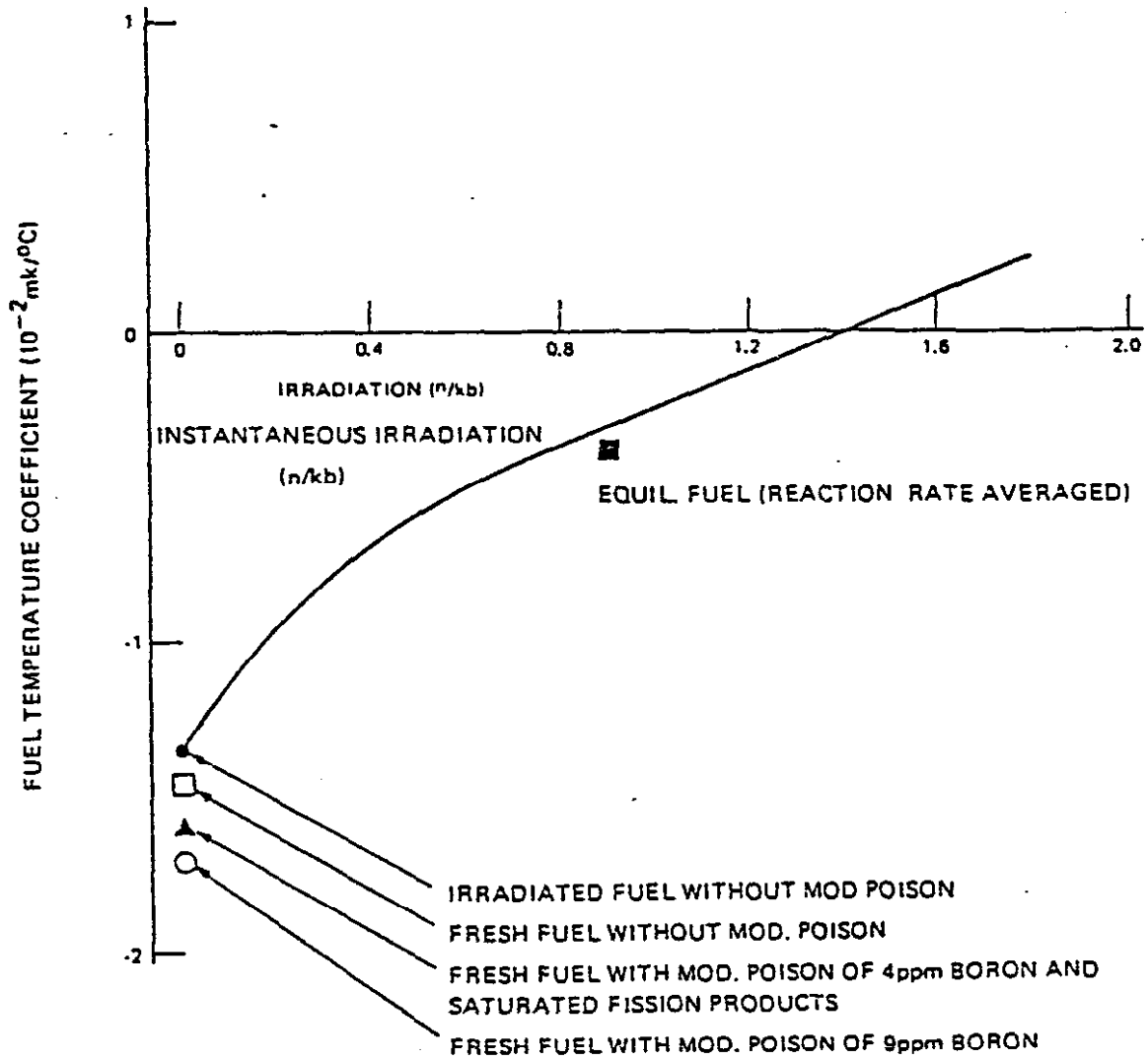
FIGURE 3.2-14   FUEL TEMPERATURE REACTIVITY COEFFICIENT
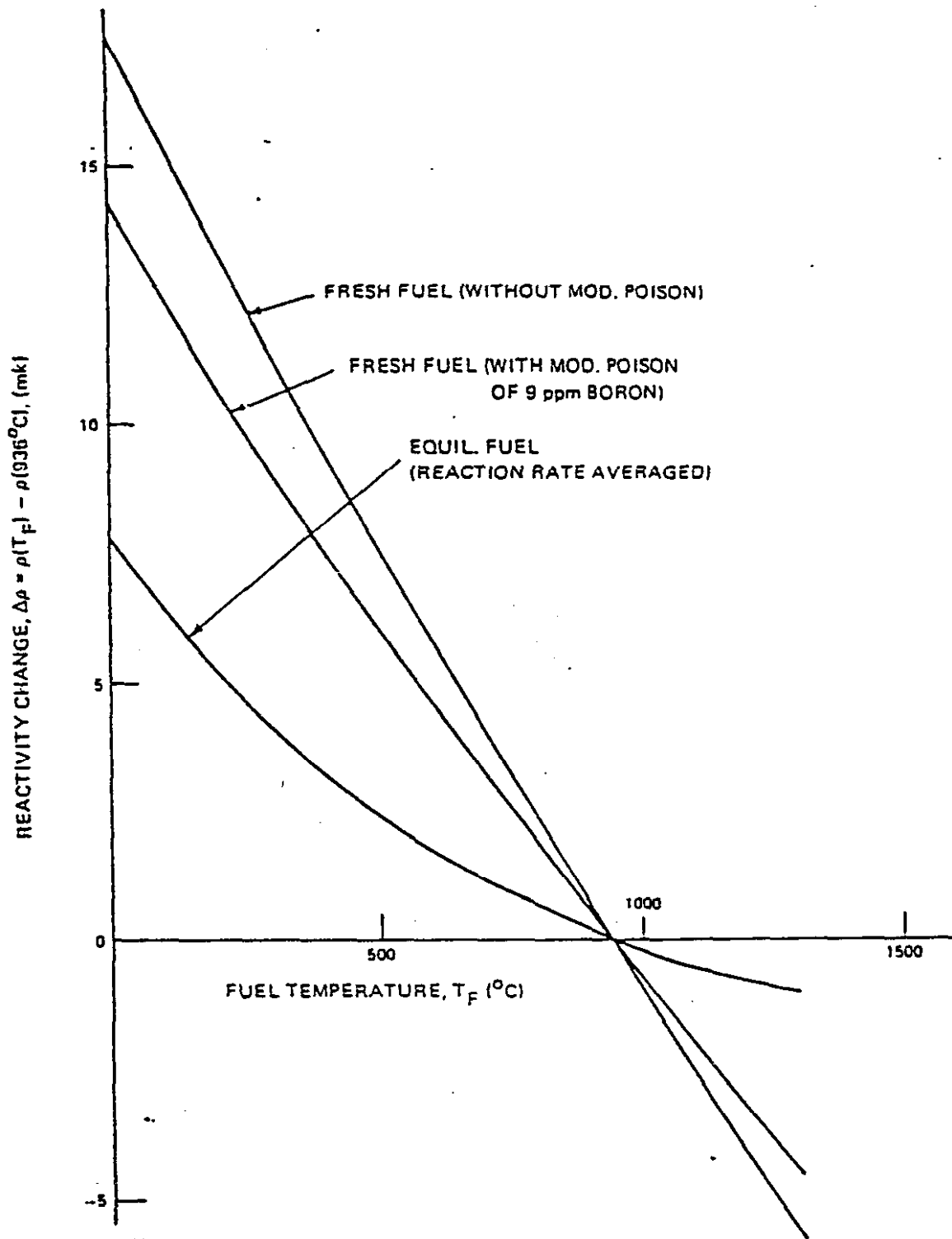
FIGURE 3.2-15   REACTIVITY CHANGE DUE TO CHANGING THE FUEL TEMPERATURE
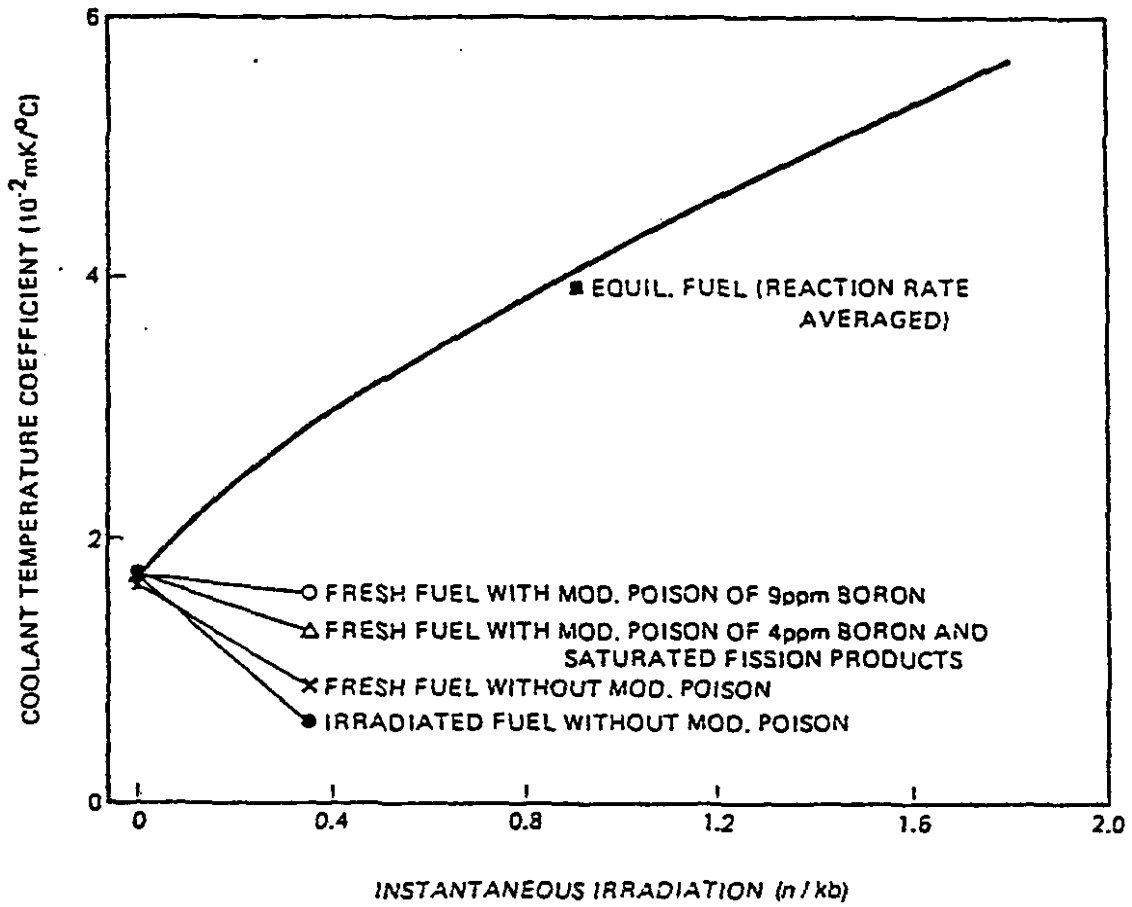
FIGURE 3.2-16   COOLANT TEMPERATURE COEFFICIENT
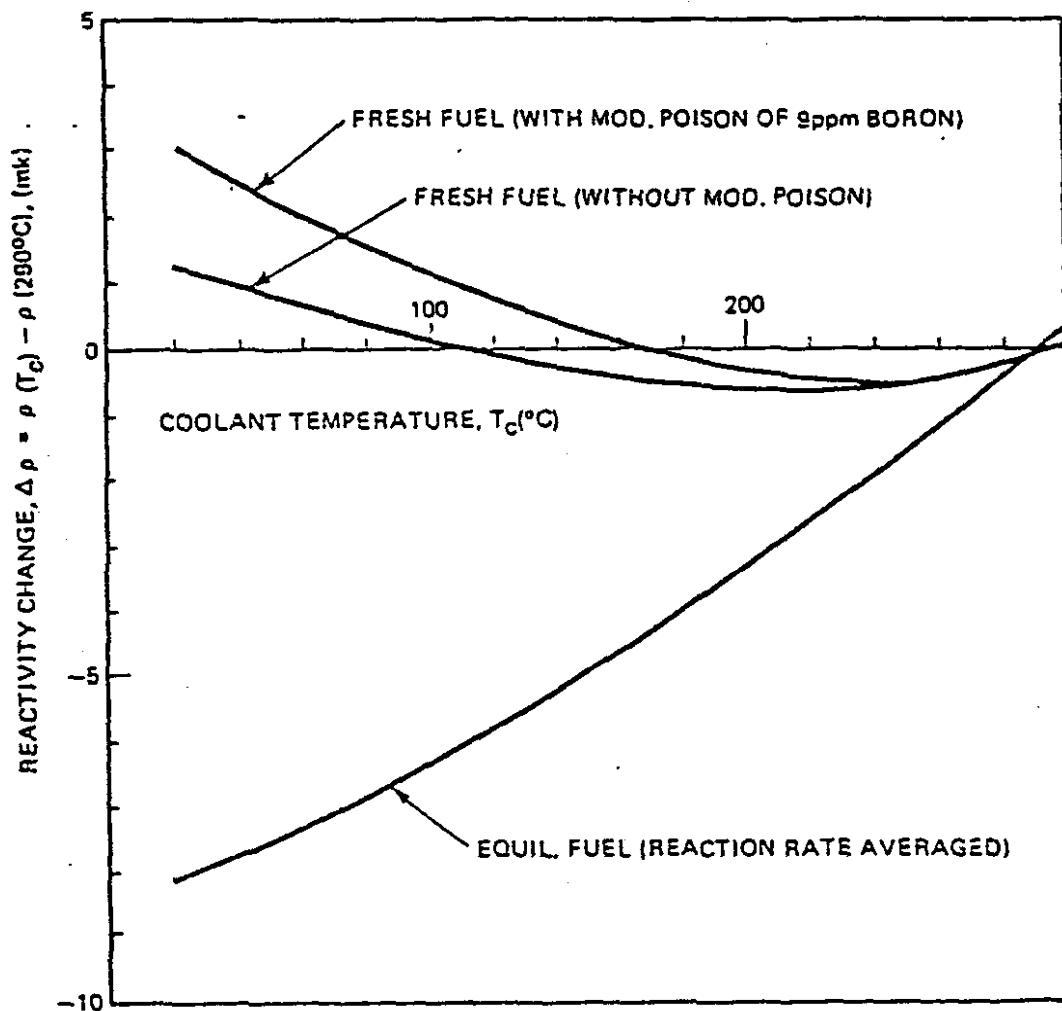
FIGURE 3.2-17   REACTIVITY CHANGE DUE TO CHANGE IN COOLANT
TEMPERATURE INCLUDING DENSITY EFFECT
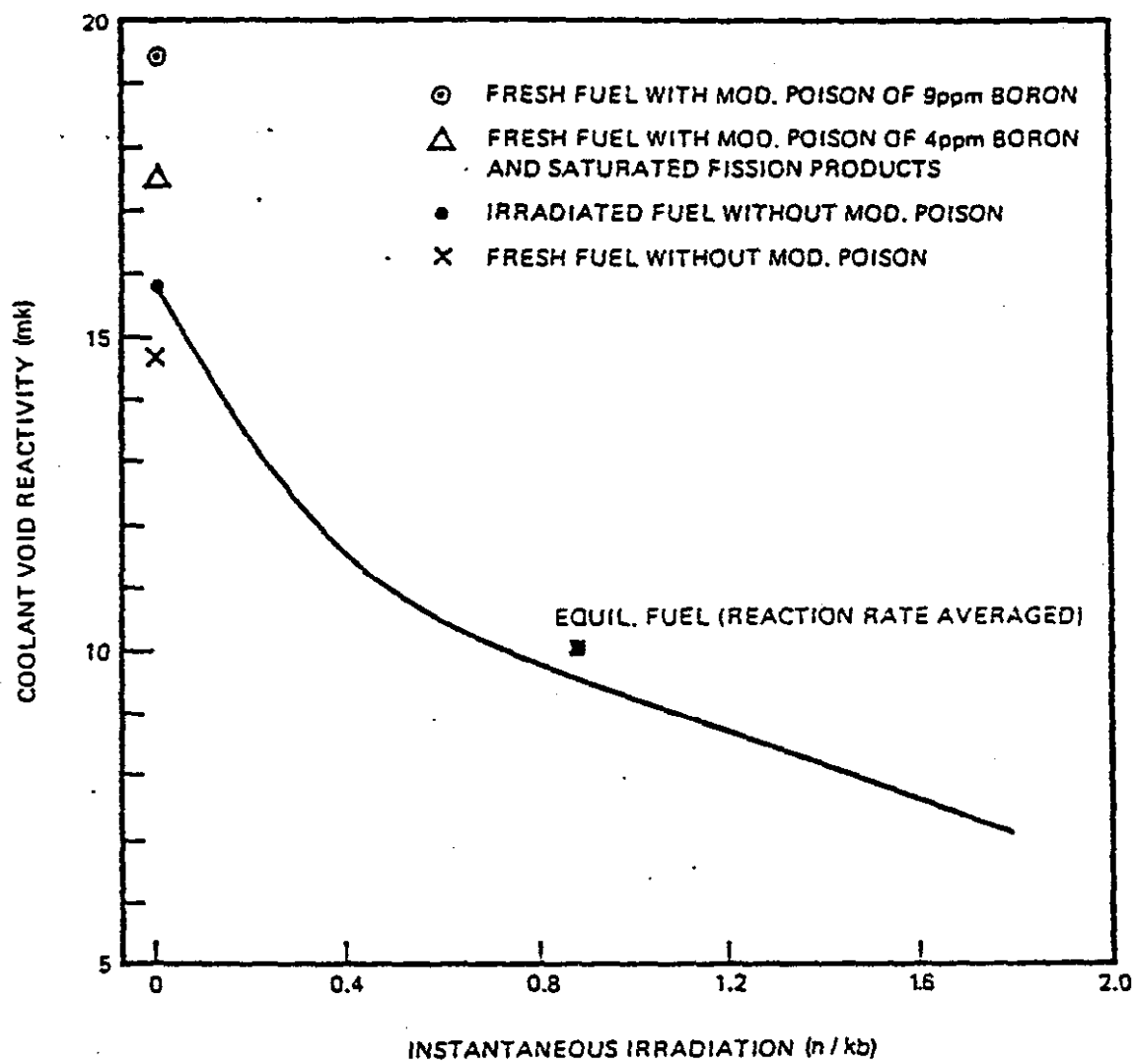
FIGURE 3.2-18   COOLANT VOID REACTIVITY AT FULL POWER
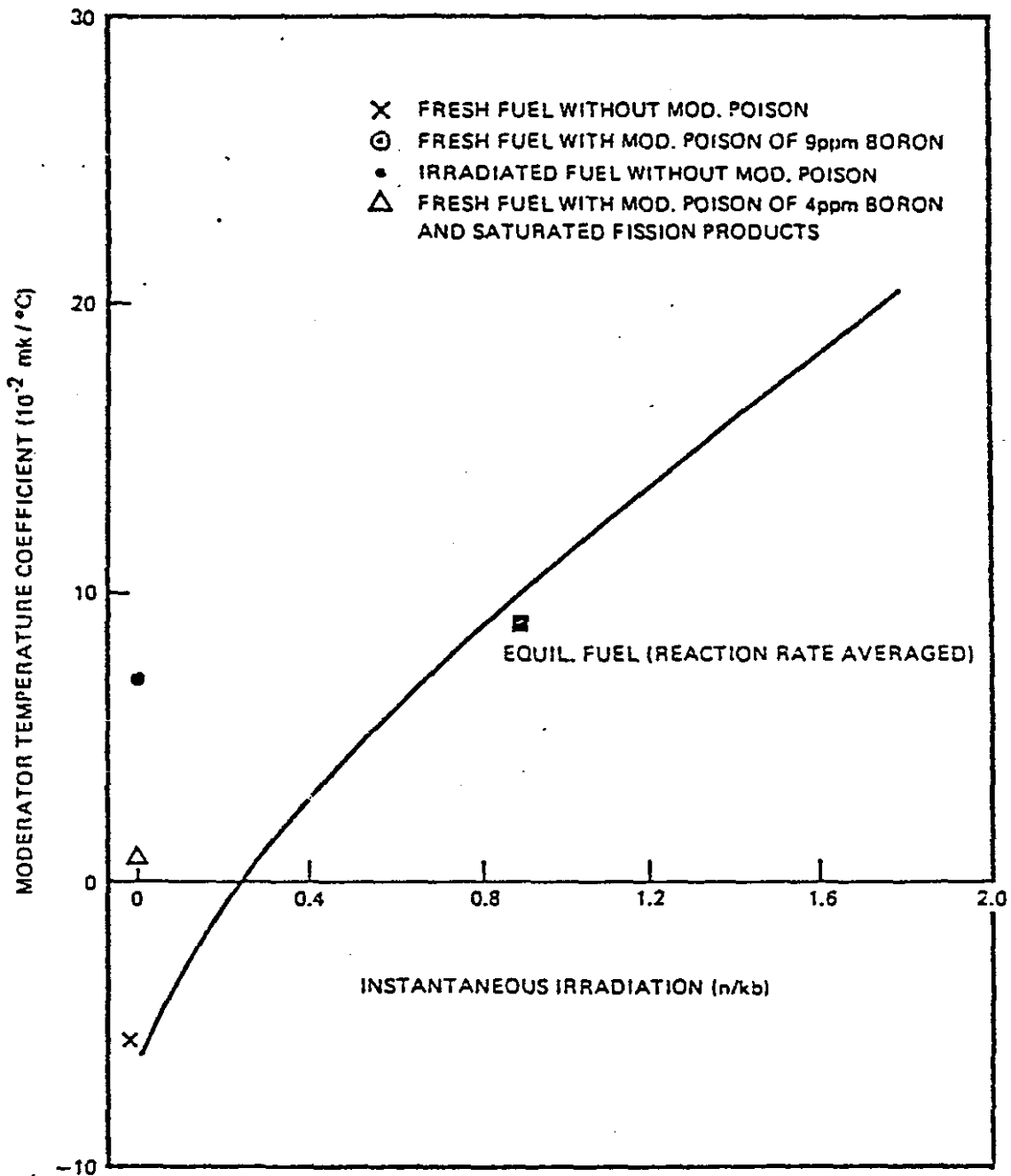
FIGURE 3.2-19　MODERATOR TEMPERATURE COEFFICIENT AT FULL POWER
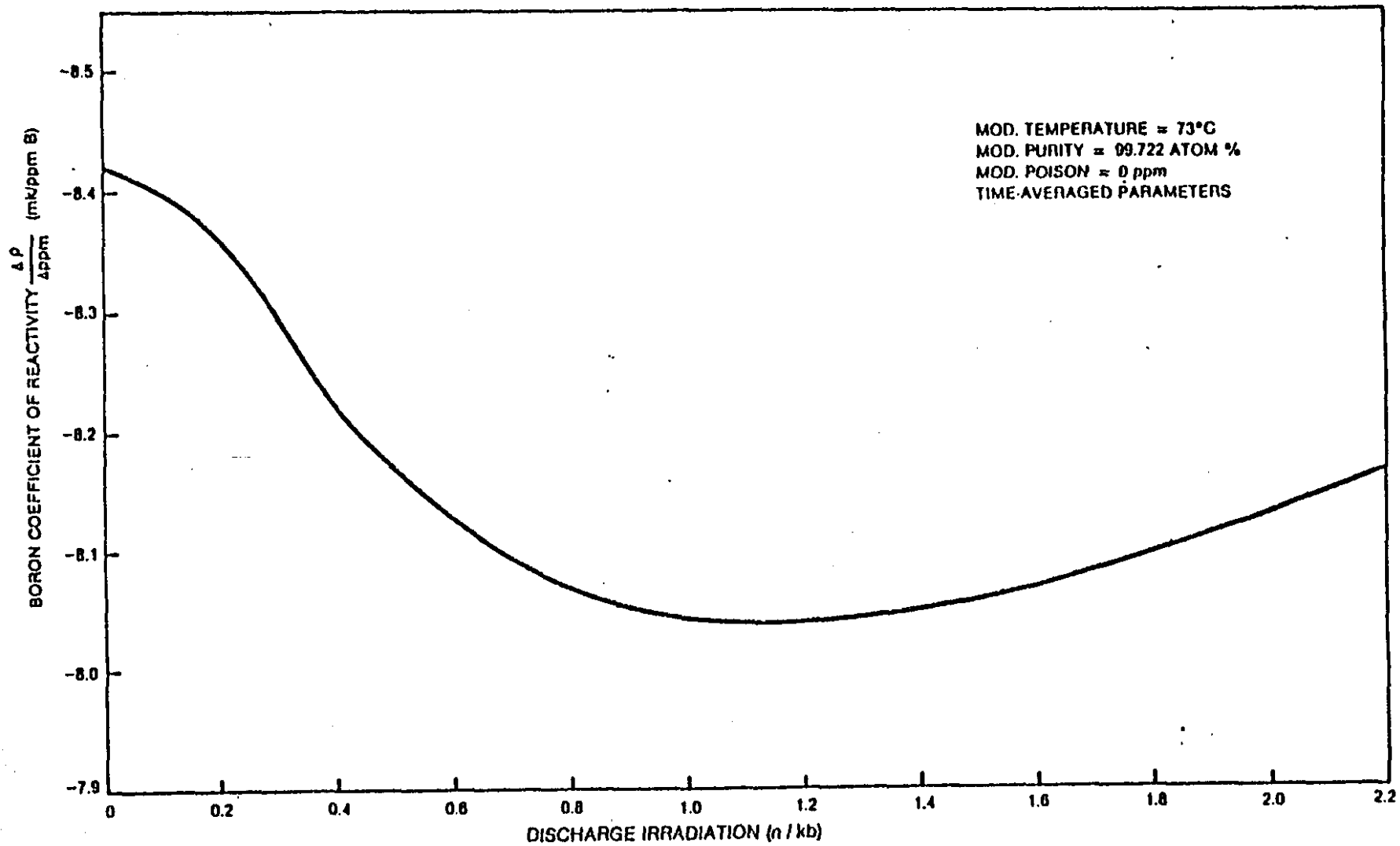
FIGURE 3.2-20   VARIATION OF BORON COEFFICIENT WITH IRRADIATION
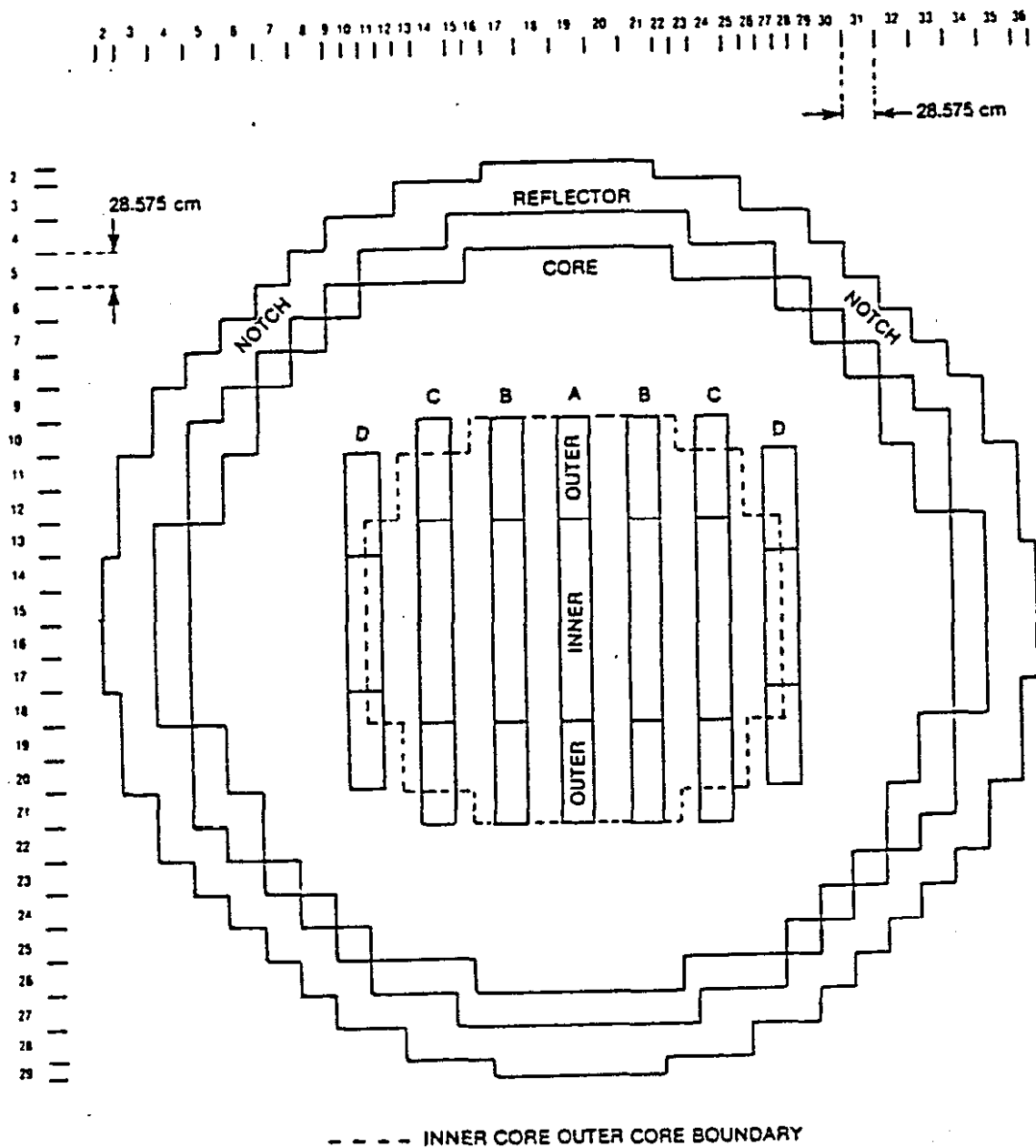
FIGURE 3.2-21   600 MW REACTOR MODEL FACE VIEW SHOWING ADJUSTER
ROD TYPES
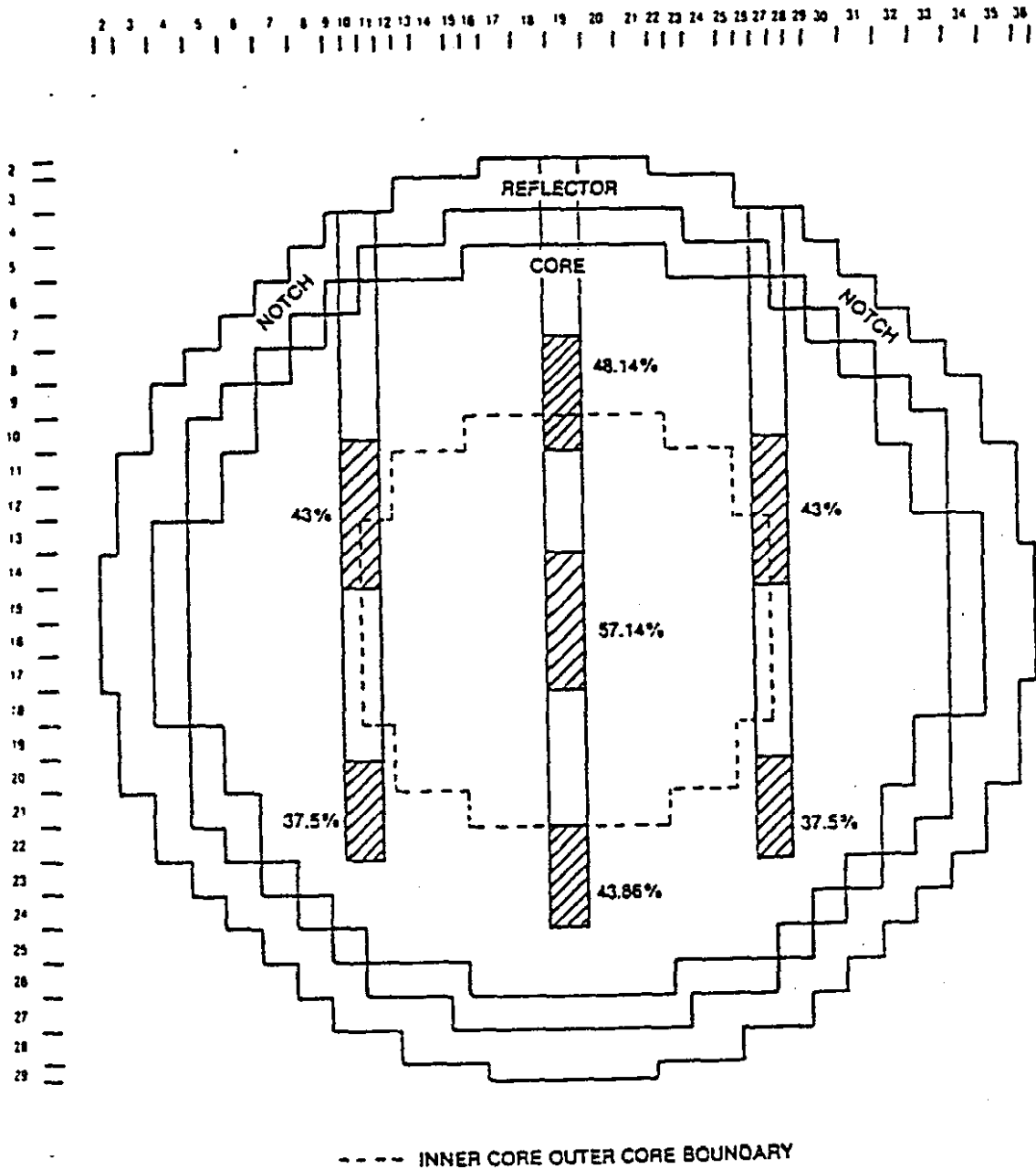
FIGURE 3.2-22   600 MW REACTOR MODEL FACE VIEW SHOWING ZONE
CONTROLLERS AND WATER LEVELS ASSUMED
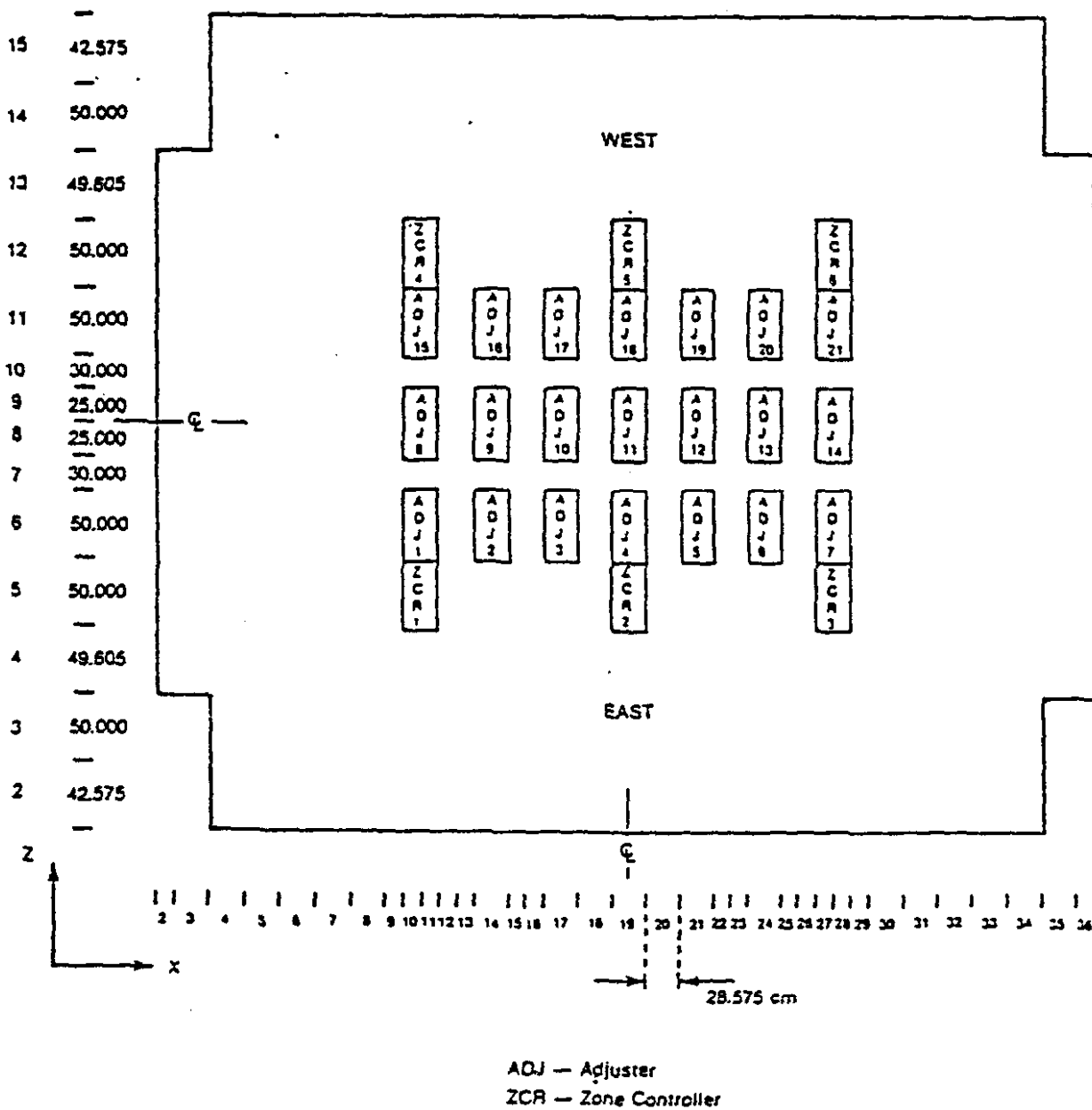
FIGURE 3.2-23   600 MW REACTOR MODEL
Top view showing adjuster and zone controller locations
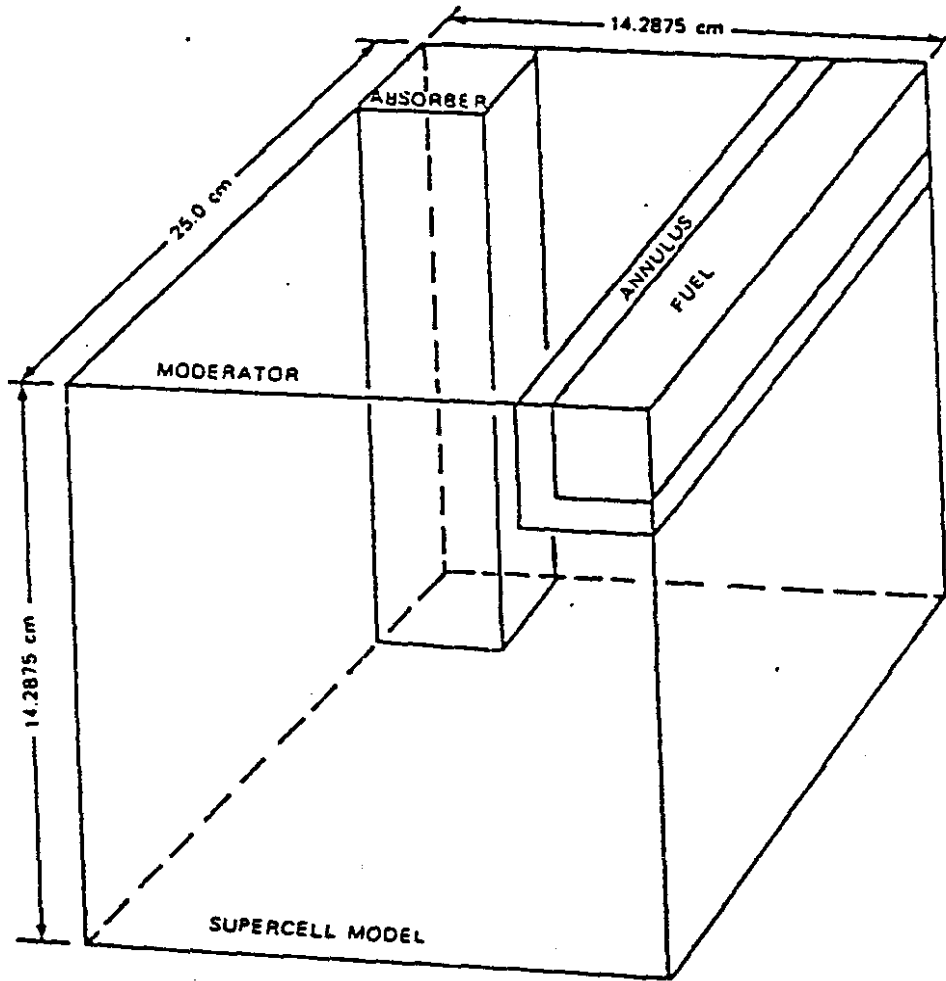
FIGURE 3.2-24 TYPICAL SUPERCELL MODEL
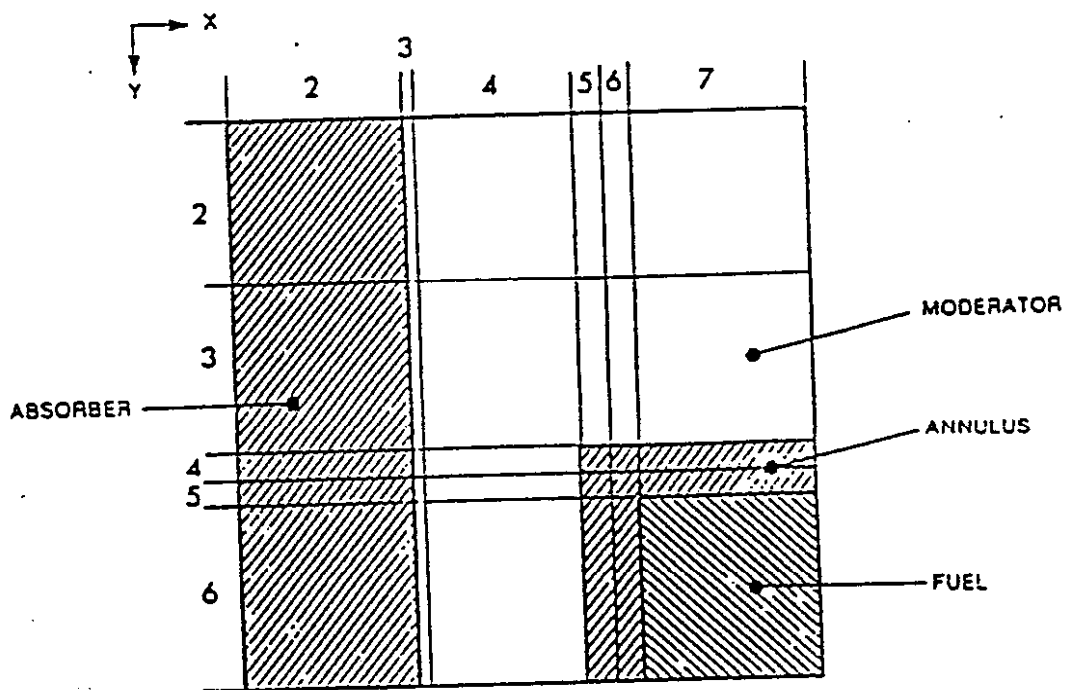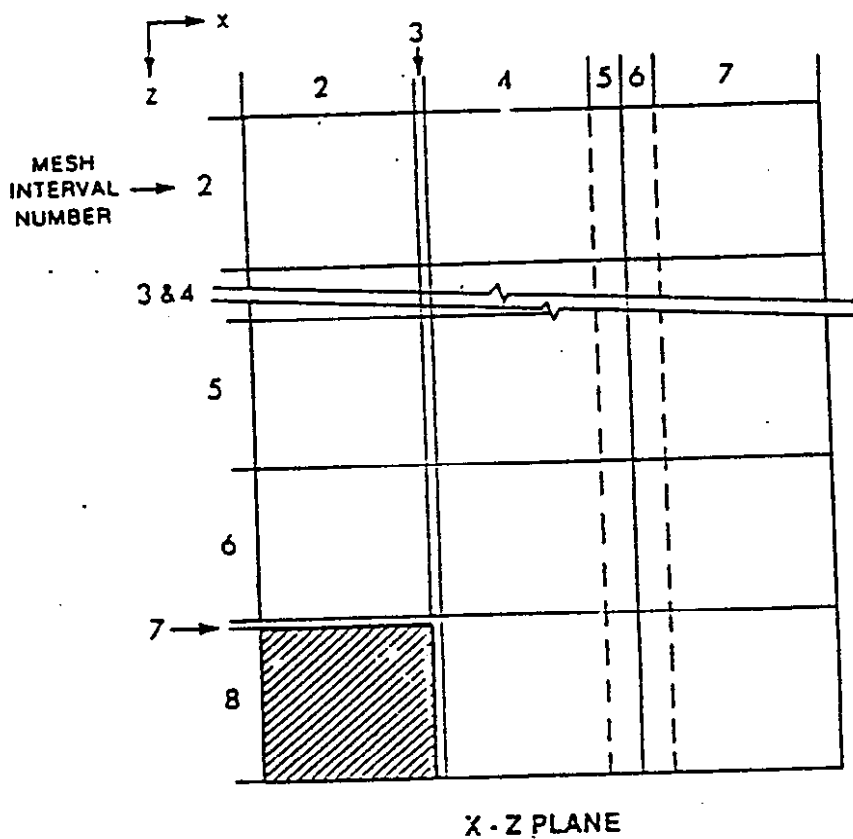
FIGURE 3.2-25   MODEL USED IN SAMPLE CALCULATION
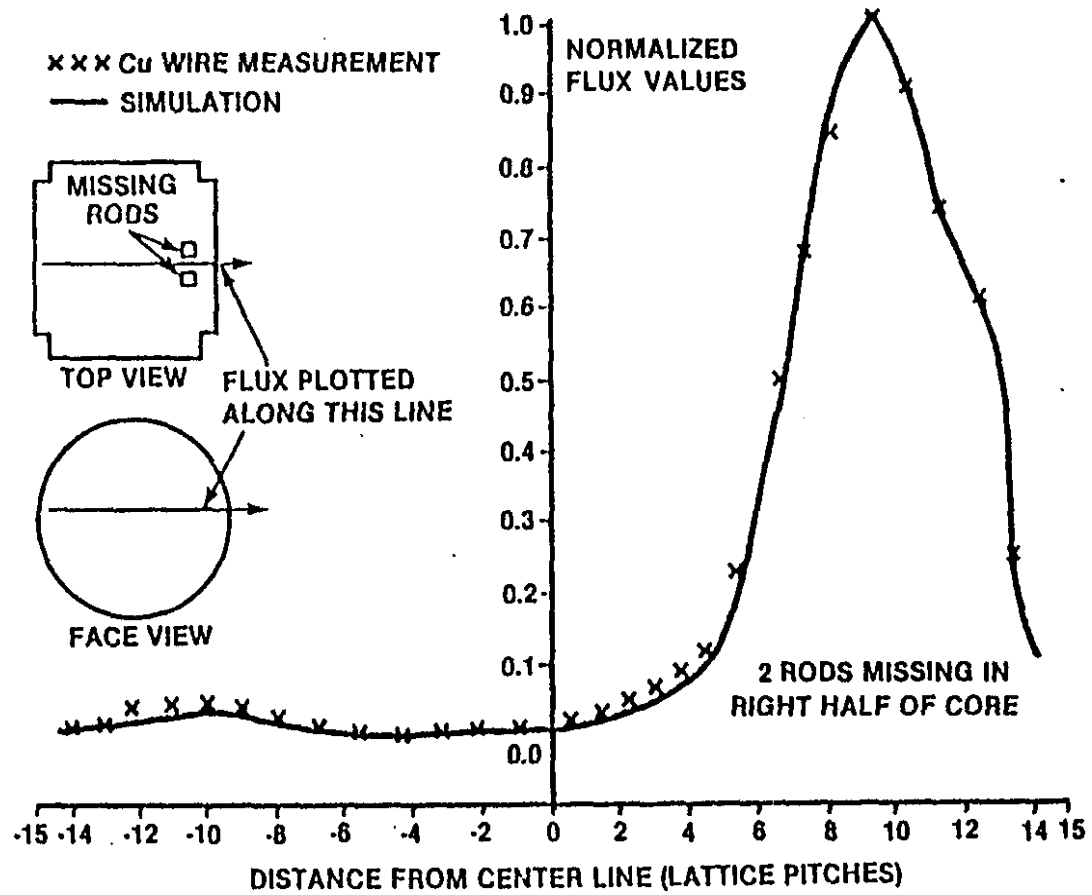
FIGURE 3.2-26   COMPARISON BETWEEN MEASURED AND CALCULATED RADIAL FLUX DISTRIBUTION IN
THE BRUCE CORE WITH 28 SHUTOFF UNITS ASYMMETRICALLY INSERTED
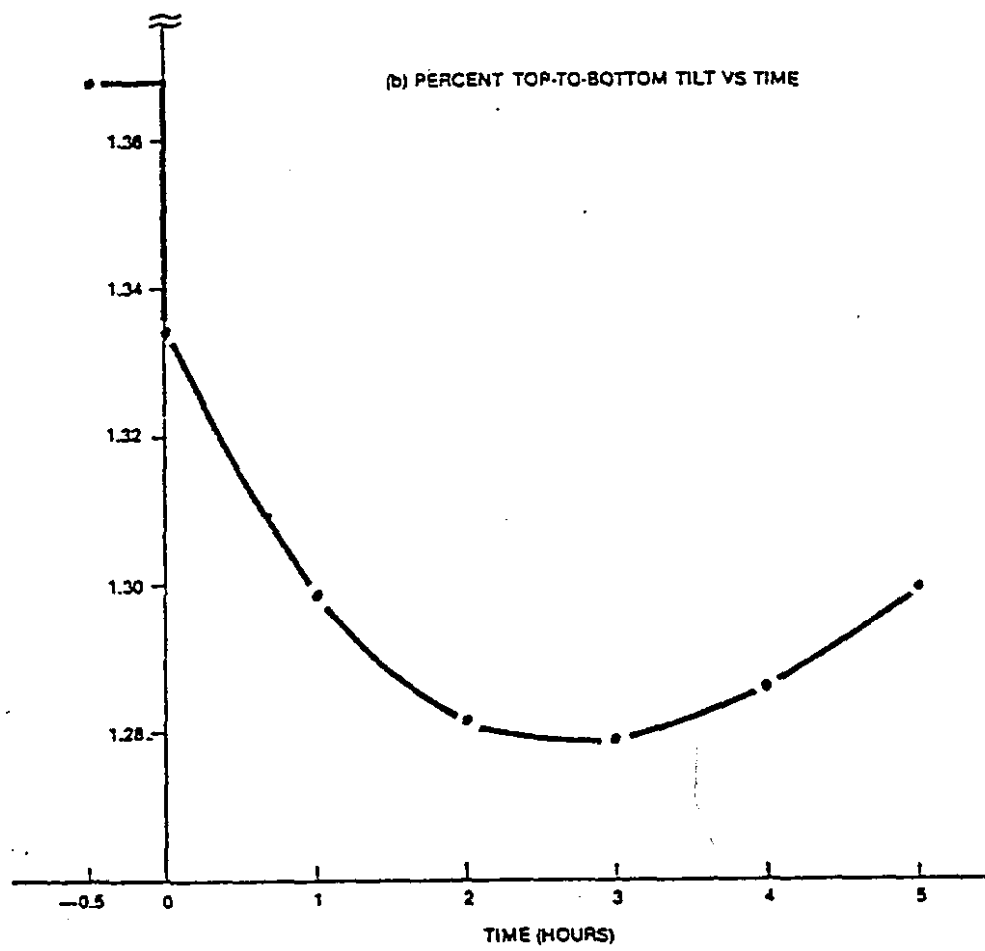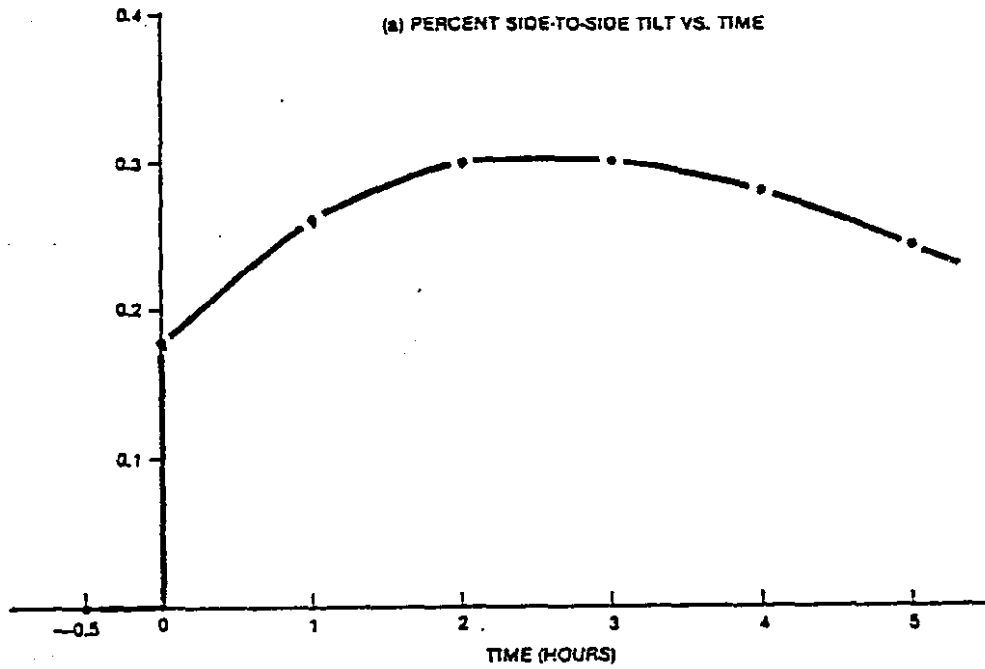
FIGURE 3.2-27   TRANSIENT AFTER A REFUELLING PERTURBATION, ZONE CONTROL
                SYSTEM OPERATING
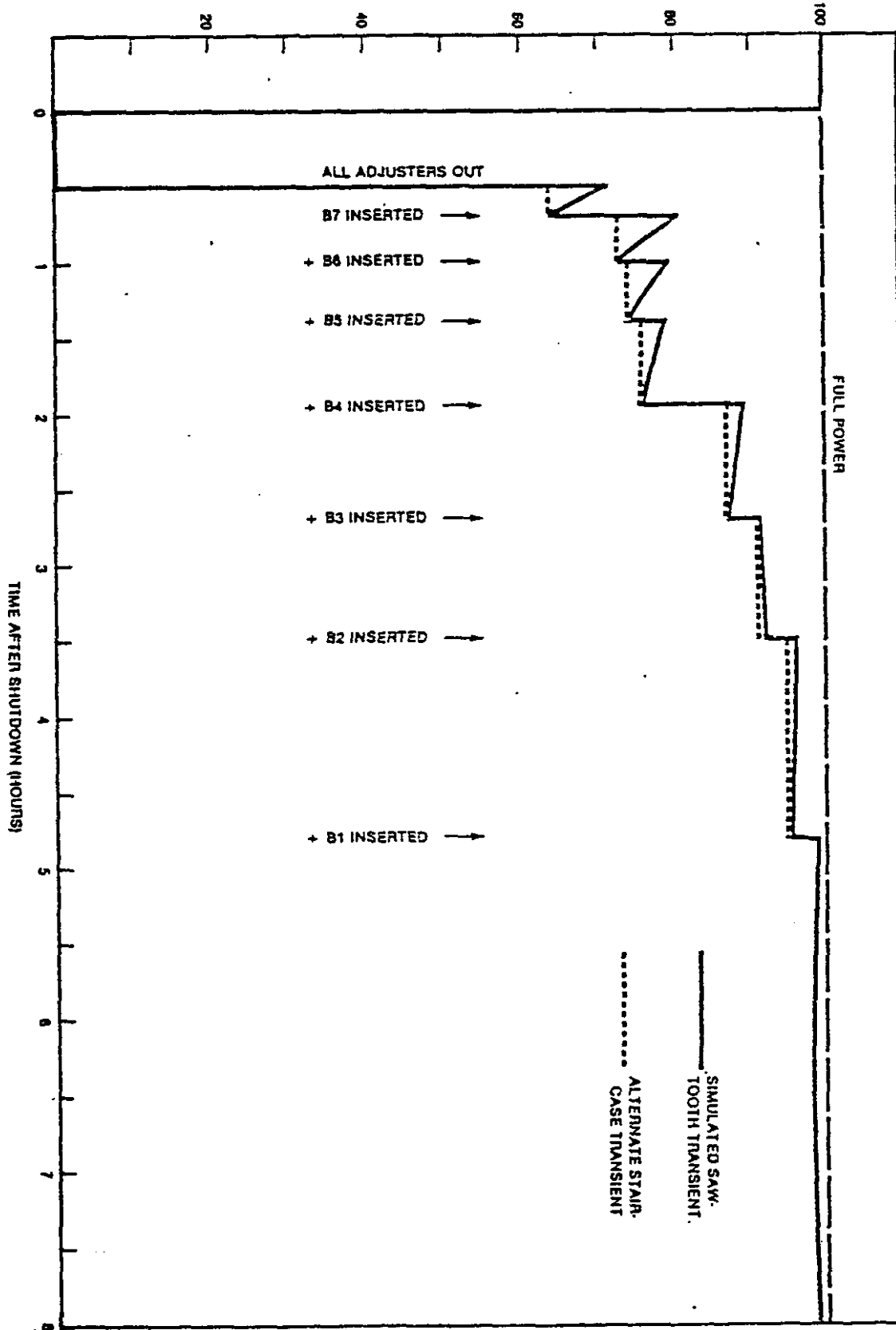
FIGURE 3.2.28   REACTOR POWER TRANSIENT DURING A STARTUP FOLLOWING A 30 MIN. SHUTDOWN

CONE
SHAPED
JETS
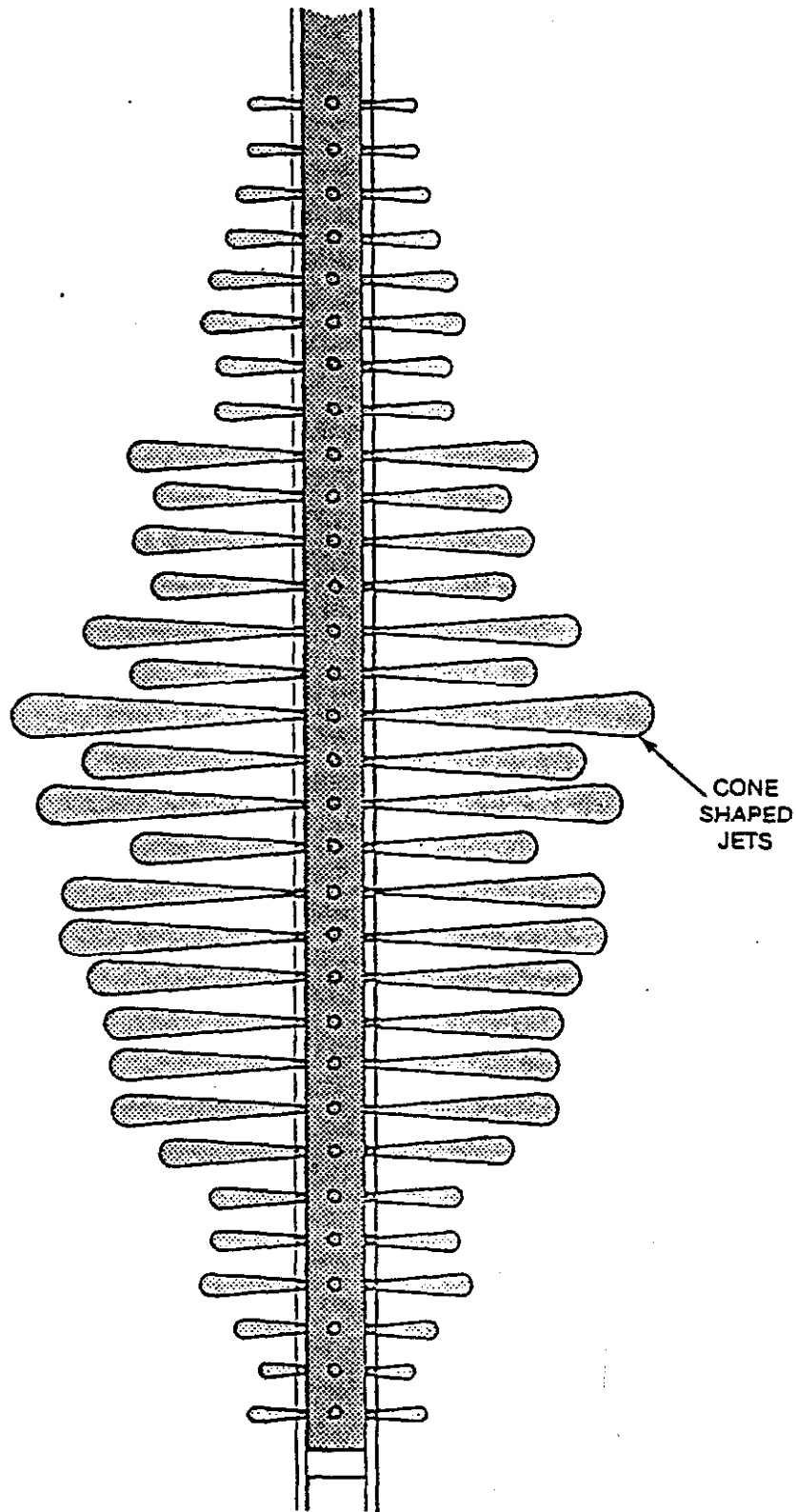
FIGURE 3.2-29 POISON INJECTION NOZZLES

MODEL SIDE VIEW AT 0.5 SEC (NOZZLE INLET END) — TOP / BOTTOM
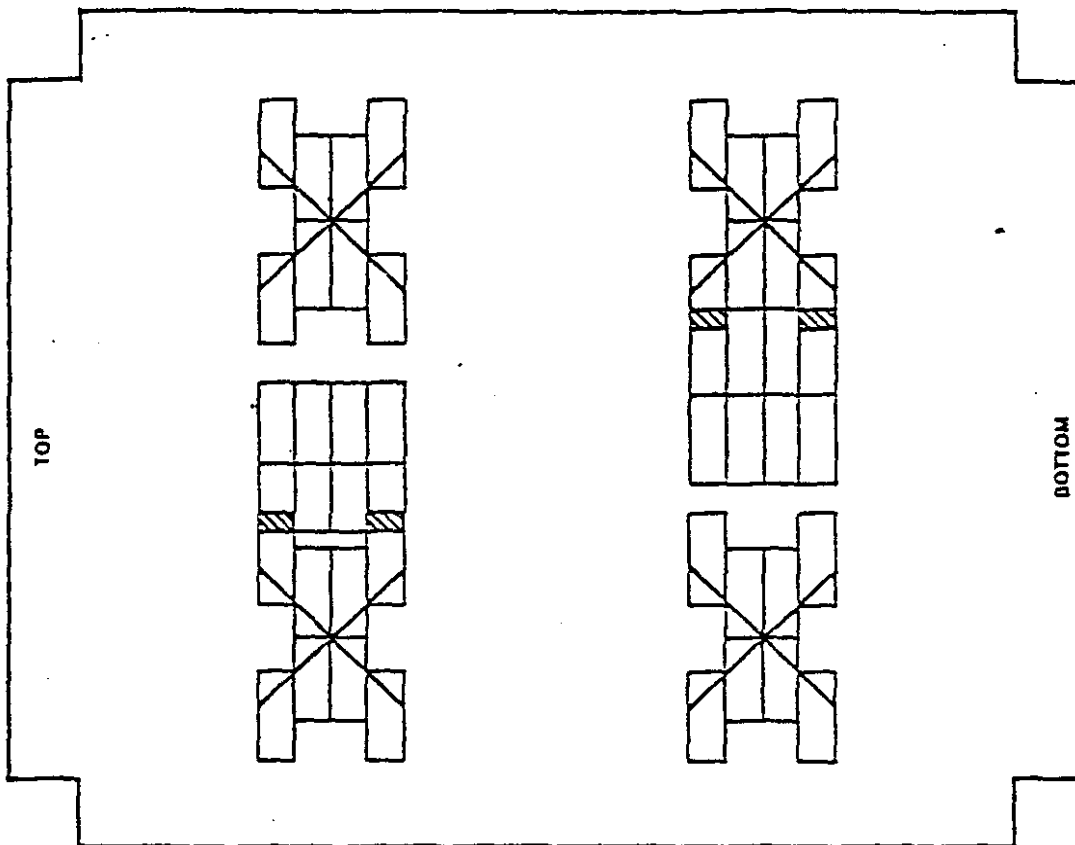
MODEL SIDE VIEW AT 0.35 SEC. (NOZZLE INLET END) — TOP / BOTTOM

28.575 cm

50 cm.
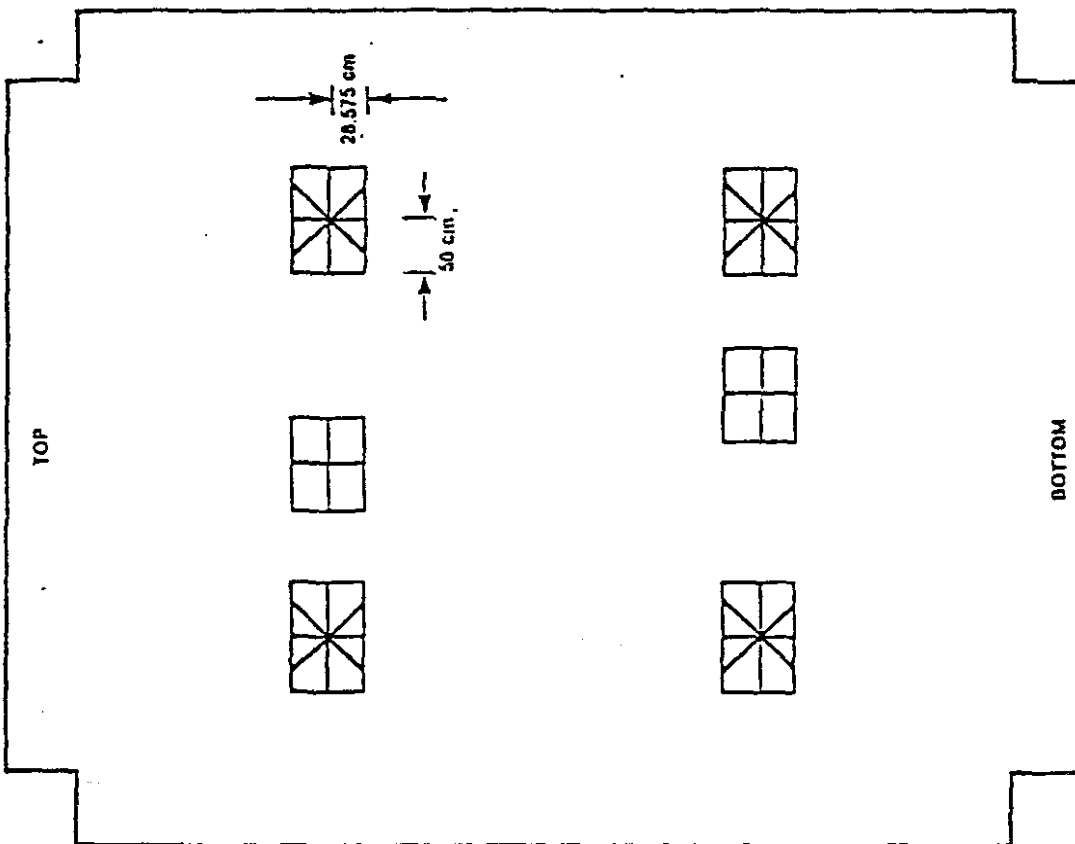
FIGURE 3.2-30 CHEBY FULL CORE MODEL USED FOR STUDYING WORTH OF POISON INJECTION SYSTEM

TDAI-244
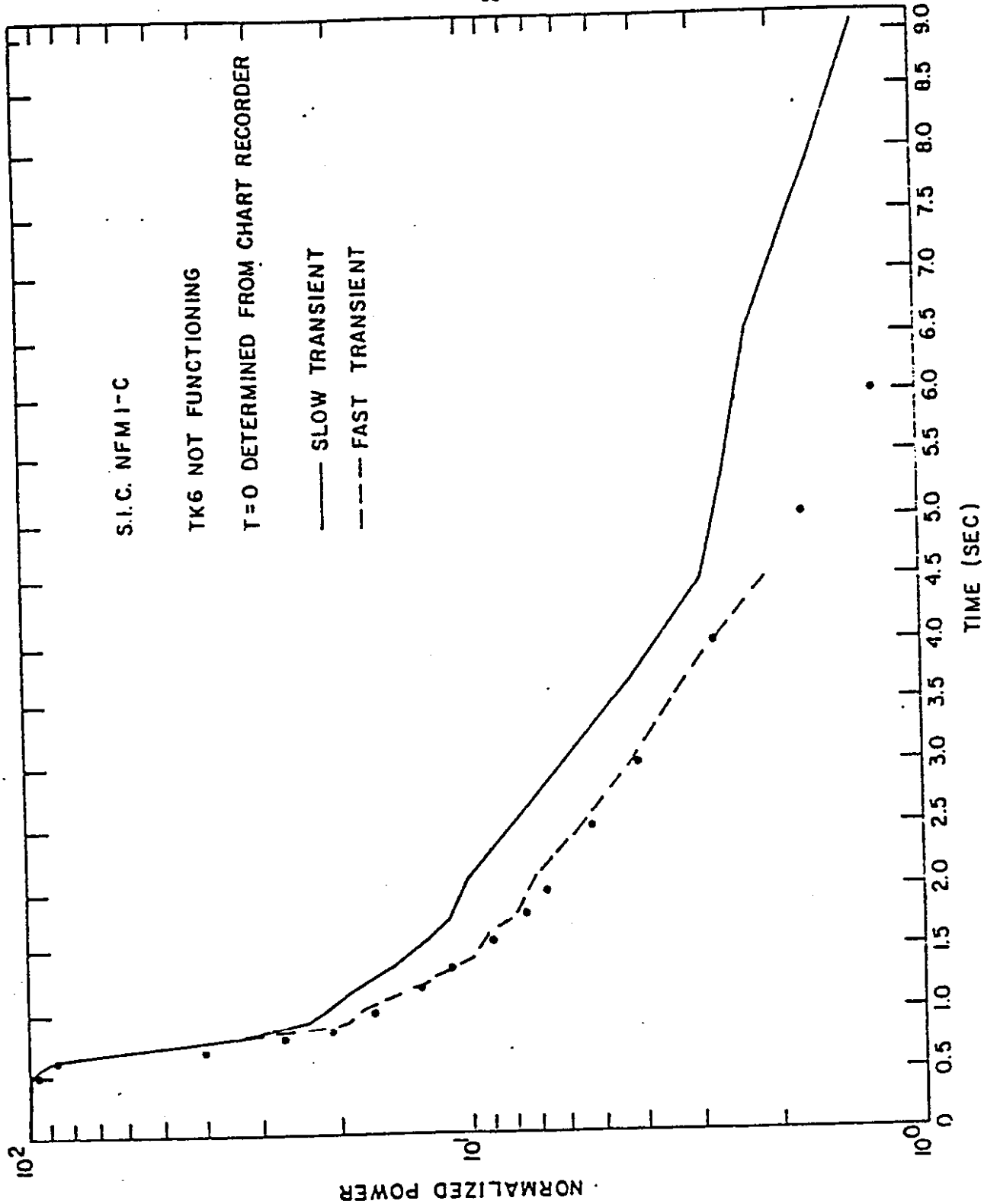
FIGURE 3.2-31   SDS 2 TEST-6 TANKS   TEST — 6 TANKS

STEAM PIPES

STEAM GENERATORS

PRIMARY PUMPS

PRESSURIZER

HEADERS   HEADERS

CALANDRIA

REACTOR

FUEL

☐ LIGHT WATER STEAM

☐ LIGHT WATER CONDENSATE

☰ HEAVY WATER COOLANT

☐ HEAVY WATER MODERATOR

MODERATOR PUMP

MODERATOR HEAT EXCHANGER
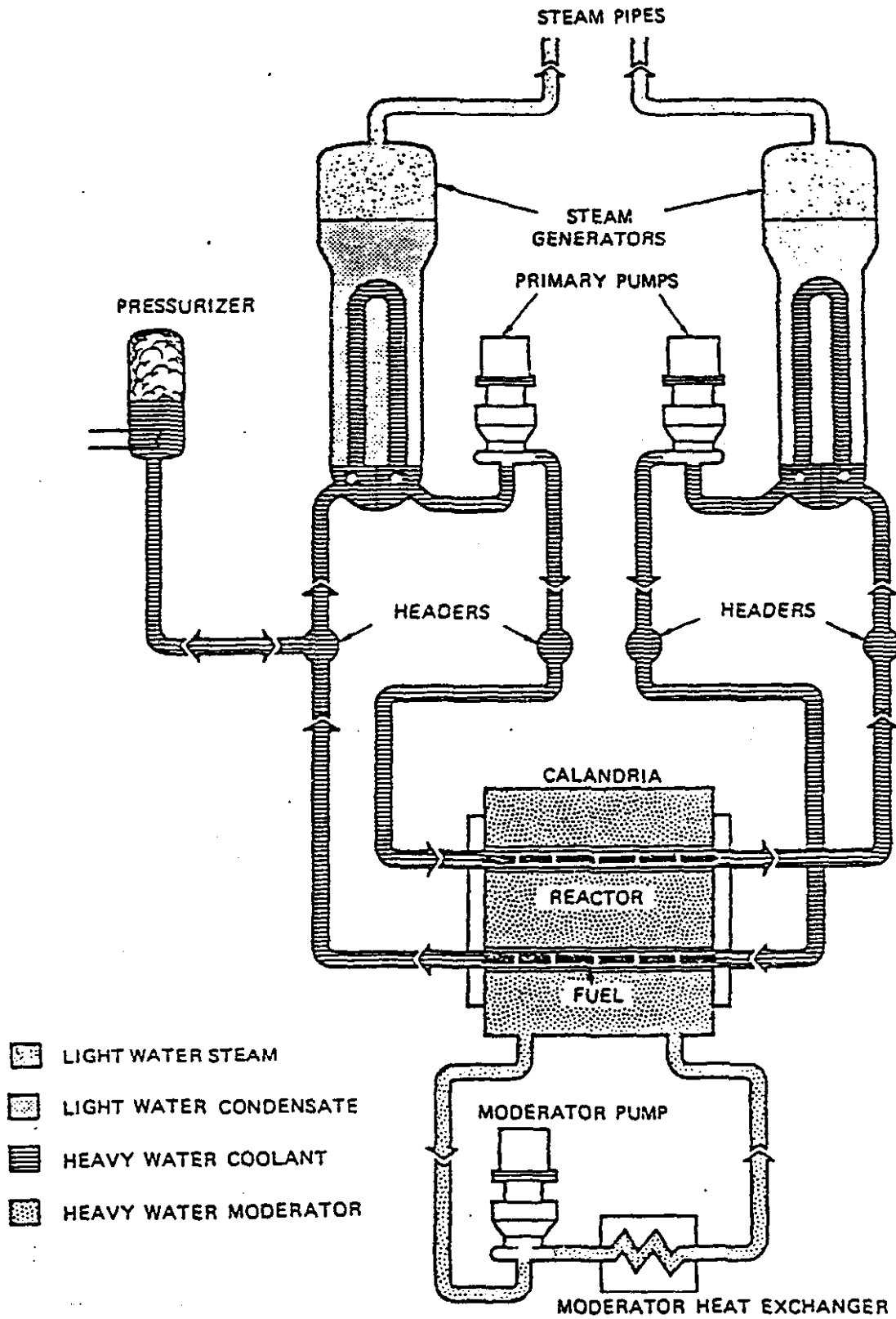
FIGURE 3.2-32 CANDU RECTOR — SIMPLIFIED FLOW DIAGRAM
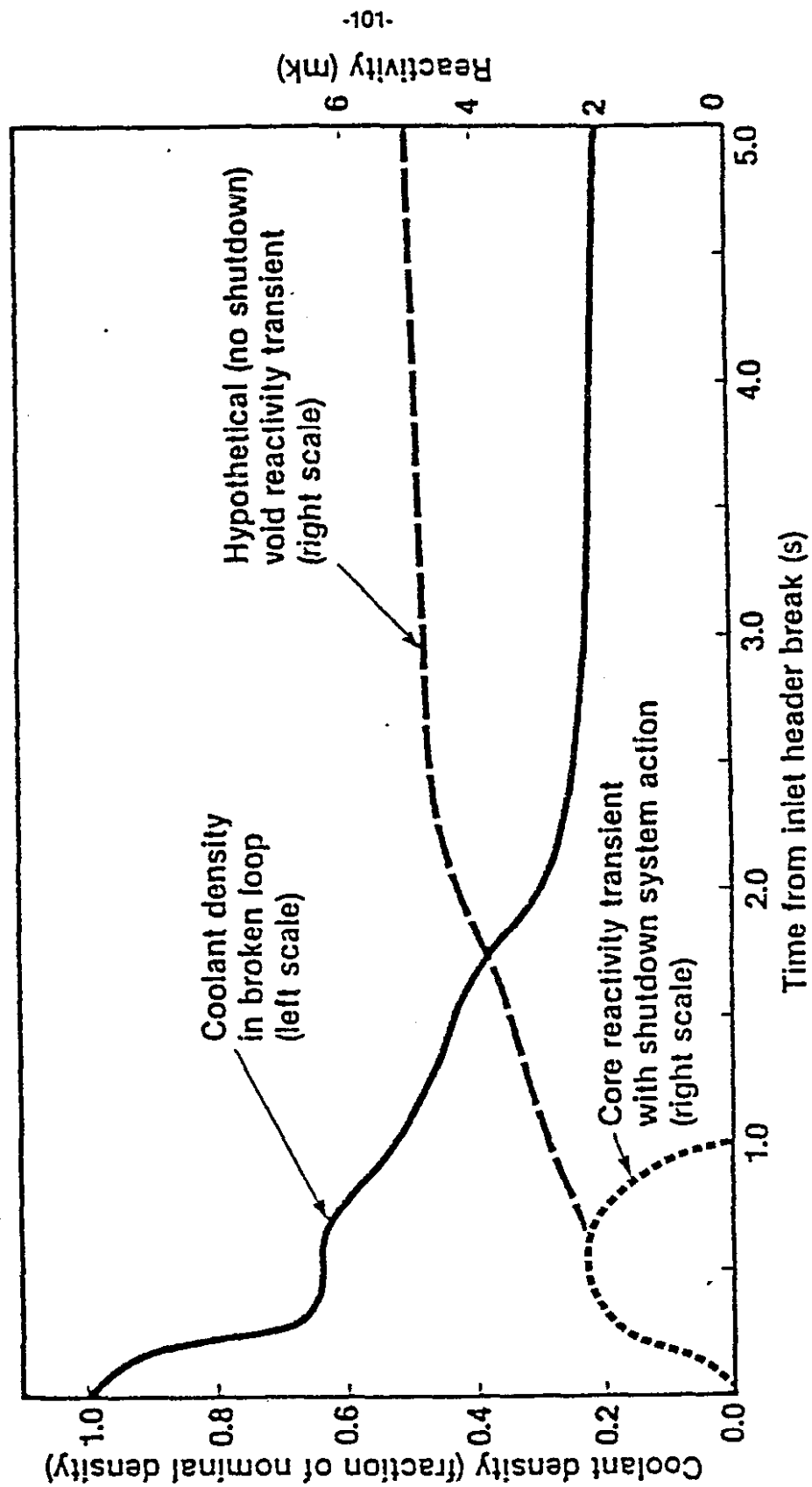
FIGURE 3.2-33   COOLANT DENSITY CHANGE AND CORE REACTIVITY
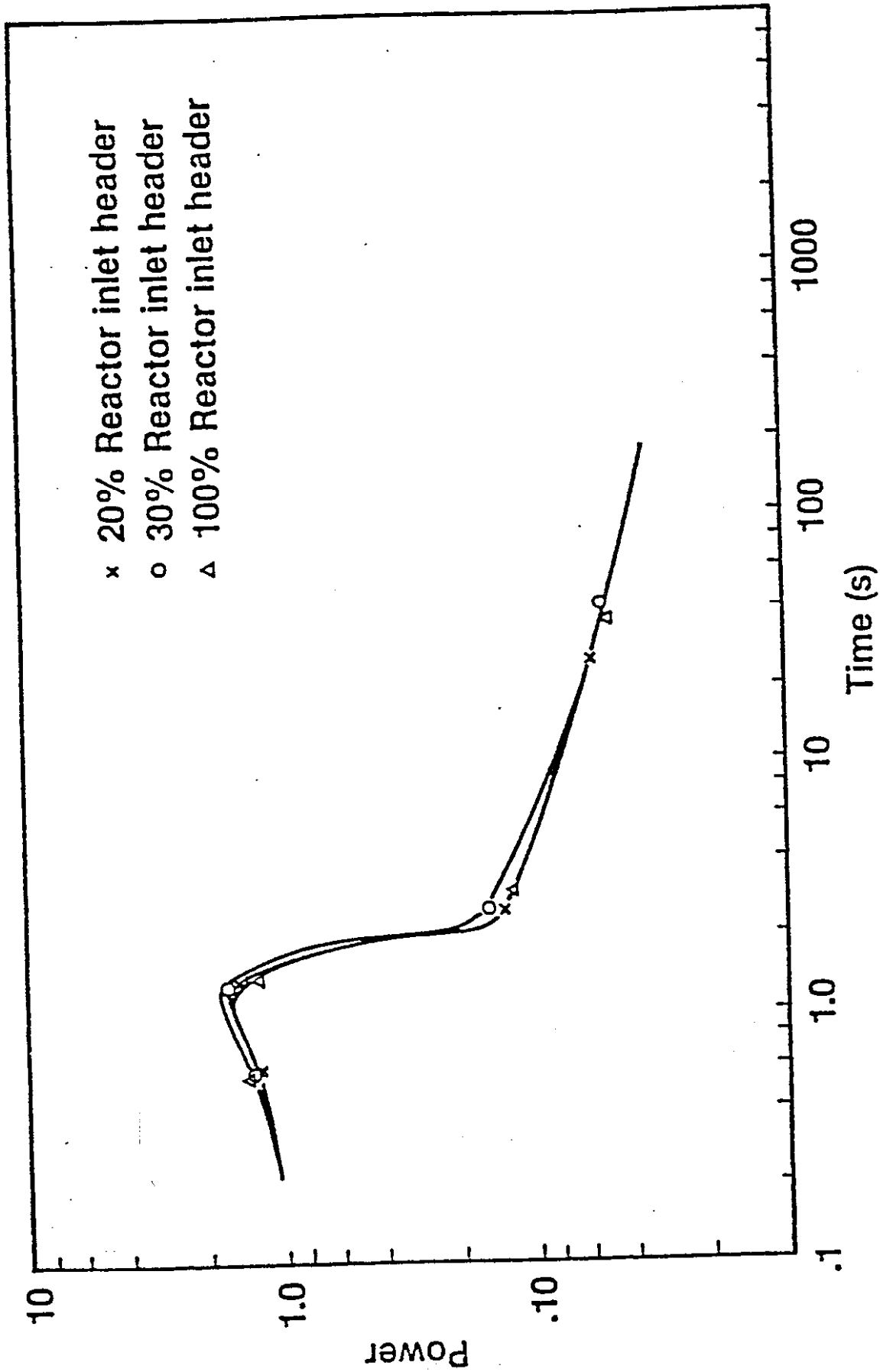FOR 100% BREAK IN INLET HEADER
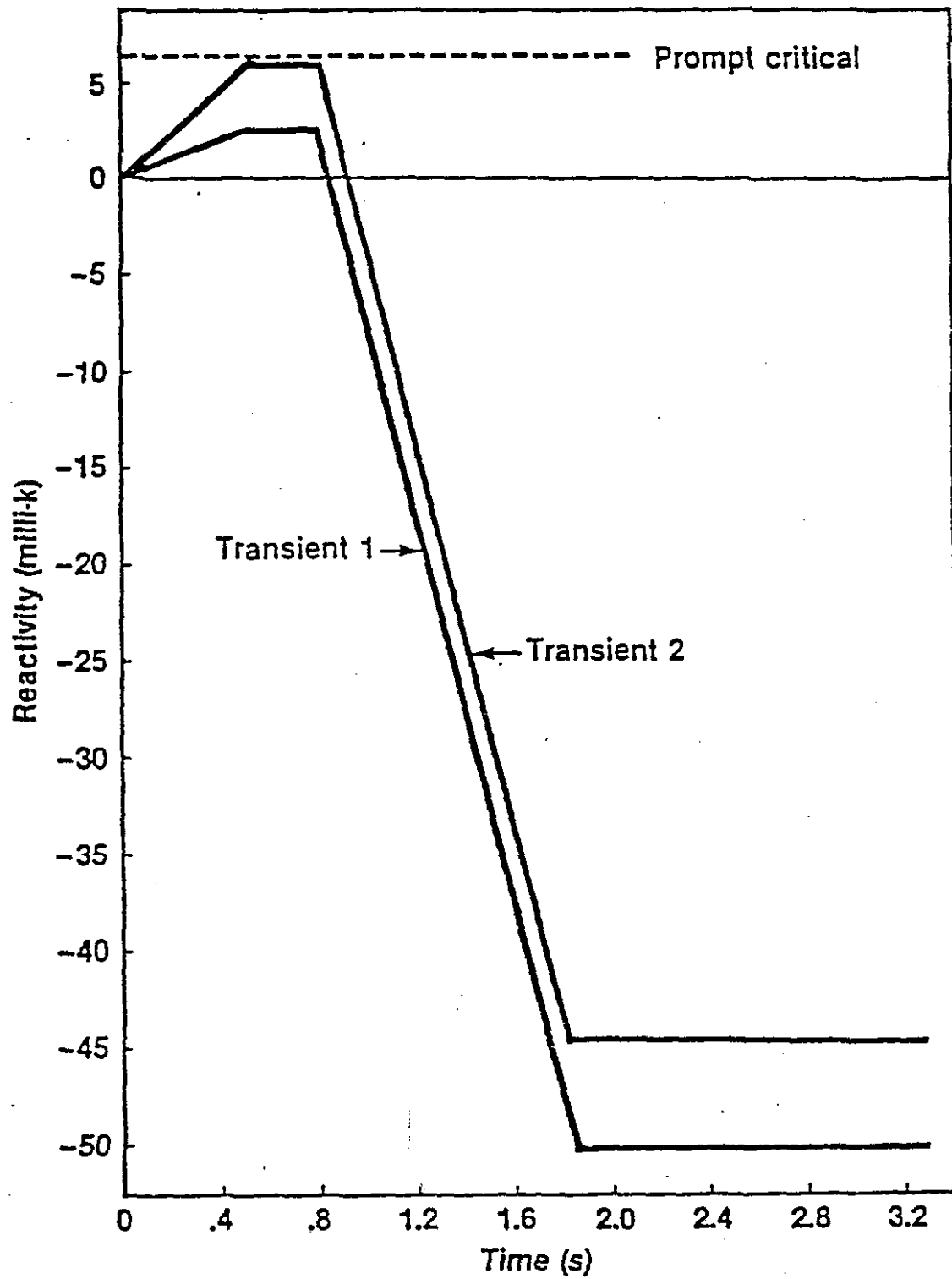
-201-

FIGURE 3.2-34   HOT BUNDLE POWER TRANSIENT

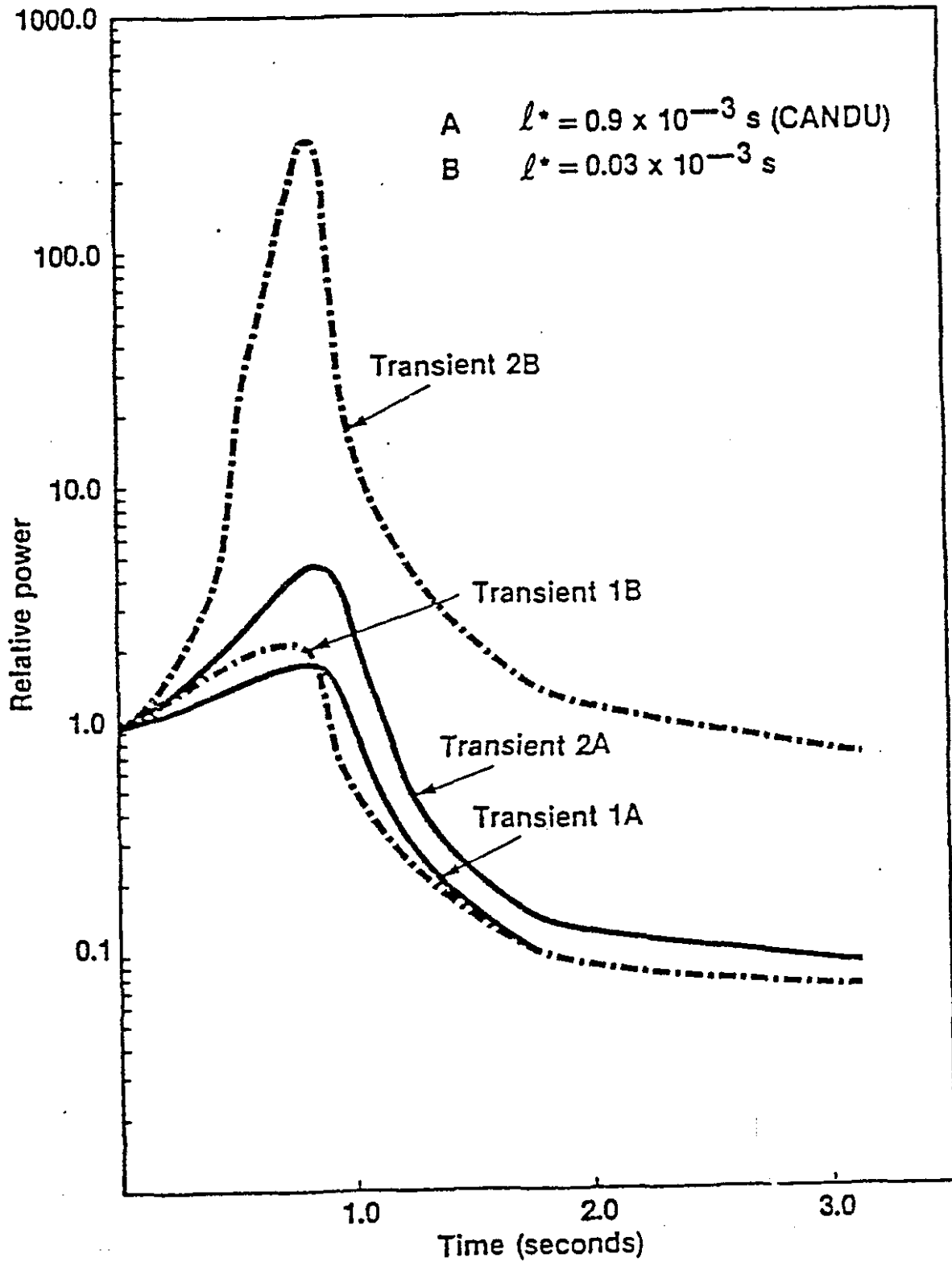FIGURE 3.2-35   HYPOTHETICAL REACTIVITY EXCURSIONS

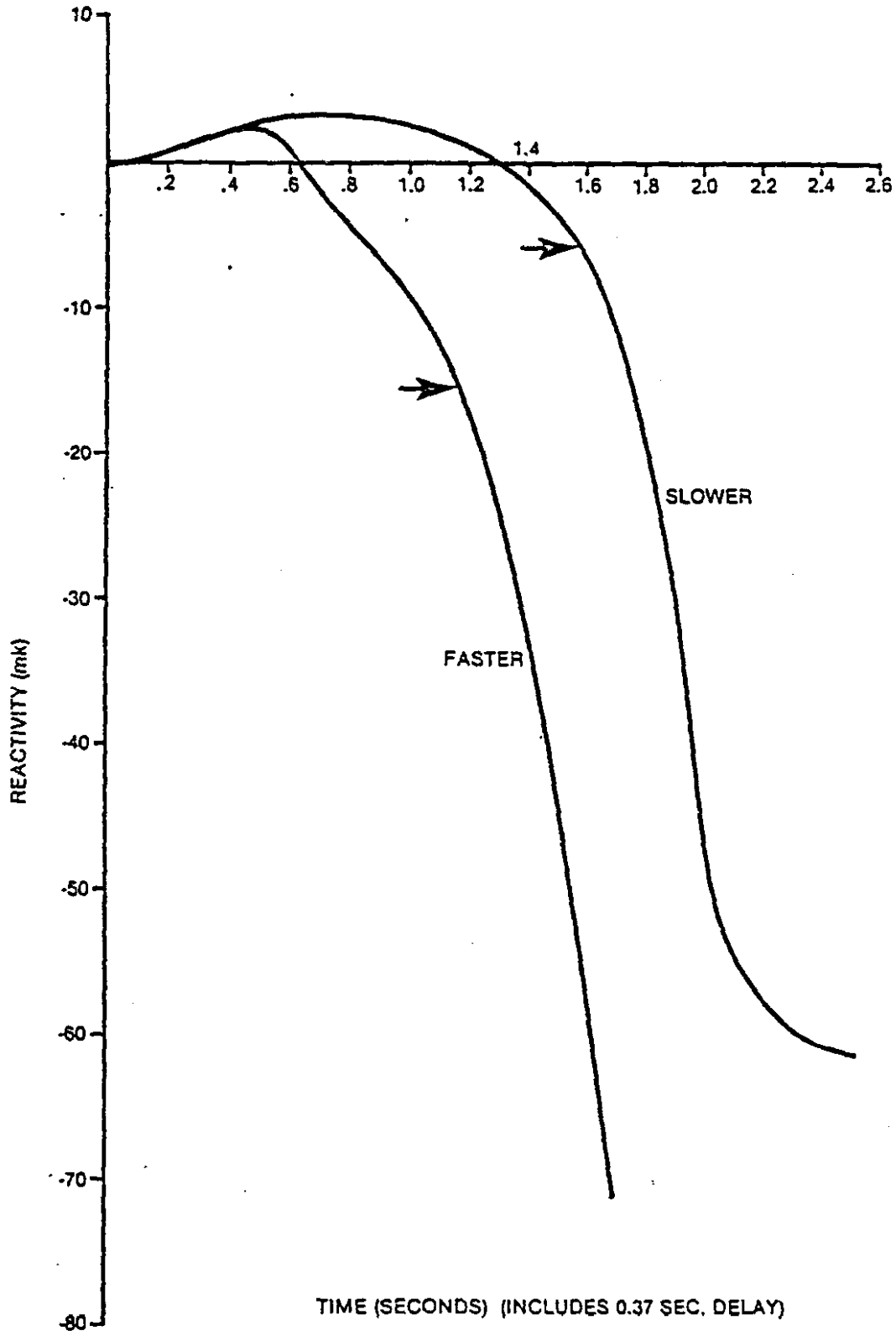FIGURE 3.2-36   SENSITIVITY OF POWER EXCURSION TO ℓ^*

FIGURE 3.2-37   DYNAMIC SYSTEM REACTIVITY VS TIME
AFTER INLET HEADER BREAK